

# NMR Spectroscopy

Pulsed NMR spectroscopy is one of the most commonly used spectroscopic tools in chemistry due to its non-destructive nature, its selectivity, and the wealth of molecular information it can provide. Using both classical descriptions, in the form of vector models, and quantum mechanical descriptions, in the form of product operators, you will learn how to predict the effect of pulses on the spin states of nuclei. With the aid of these descriptions you will learn how to chain pulses together into *pulse sequences* to manipulate the spin system and produce the type of information desired at the detector. In this process you will explore core NMR concepts, such as spin echoes and polarization transfer, which form the basis for a wide variety of pulse sequences that probe molecular structure.

## Theory – Classical Description

### Basic Principles

Protons, neutrons, and electrons exhibit the intrinsic property of spin, and specifically have a spin quantum number ( $I$ ) of  $\frac{1}{2}$ . You have already encountered this with electrons; for example, populating the electronic ground state of atoms by placing two electrons as “paired” antiparallel spins in each atomic orbital. Protons and neutrons behave similarly and will generally pair up (protons pair with protons, and neutrons pair with neutrons) as antiparallel spins in the nucleus. Therefore, nuclei with an even number of protons and an even number of neutrons have  $I = 0$  since all protons are paired and all neutrons are paired, leaving no net spin angular momentum. Common examples include  $^{12}\text{C}$  with 6 protons and 6 neutrons, as well as  $^{16}\text{O}$  with 8 protons and 8 neutrons. It might then be expected that nuclei with a single unpaired proton or neutron must have  $I = \frac{1}{2}$ , but due to spin-orbit coupling this may not be the case. For example, a  $^1\text{H}$  nucleus consists of only a single proton and has  $I = \frac{1}{2}$ , but  $^{17}\text{O}$  has 9 neutrons (one unpaired) and has  $I = 5/2$ . The unpaired neutron occupies a  $d$ -type orbital which contributes 2 quanta to the total angular momentum, so the combined angular momentum is  $2 + \frac{1}{2} = 5/2$ . When there are an odd number of protons and an odd number of neutrons, the effects of the unpaired proton and unpaired neutron combine. For example, a  $^2\text{H}$  nucleus consists of both a proton and a neutron, and has  $I = 1$ . Predicting the exact value of  $I$  is generally difficult since the relative order of states does not follow a consistent pattern from one nuclide to another. However, there are some useful rules that can be derived from the logic above: 1)  $I$  is a half-integer when the mass number is odd, 2)  $I$  is an integer when the mass number is even, and 3)  $I = 0$  when the atomic number and mass number are both even.

Nuclei with  $I > 0$  have an associated angular momentum,  $P$

$$P = \hbar \sqrt{I(I+1)} \quad (1)$$

and the component on the laboratory-defined z-axis is given by

$$P_z = m_I \hbar \quad (2)$$

where  $m_I$  ranges from  $-I$  to  $I$  in integer steps and is called the magnetic quantum number. This angular momentum leads to an associated magnetic moment,  $\mu$

$$\mu = \gamma P \quad (3)$$

where  $\gamma$  is the gyromagnetic ratio, which is constant for each nuclide. The energy of a magnetic dipole in a static magnetic field (designated as  $B_0$ , which is taken to be along the z-axis) is given by

$$E_{m_I} = -\mu \cdot B_0 = -\mu_z B_0 = -\gamma B_0 m_I \hbar \quad (4)$$

Often the energy levels are expressed in terms of angular frequency units (rad/s) instead of energy (Joules), which are related by a factor of  $\hbar$ :

$$E_{m_I}/\hbar = \Omega_L m_I \quad (5)$$

where  $\Omega_L = \gamma B_0$  and is called the *Larmor frequency*.

Thus, nuclei with  $I > 0$  exhibit a splitting of energy levels when placed in an external static magnetic field based on the orientation of their spin. This effect is called the *Zeeman effect* and is analogous to the Stark effect demonstrated in the *Microwave Spectroscopy* experiment.

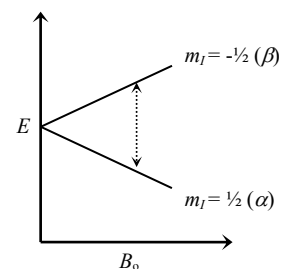


**Figure 1.** Energy level splitting as a function of the magnetic field for a nuclide with  $I = \frac{1}{2}$ .

## Single Spin of $\frac{1}{2}$

Consider the specific simple case of a single nucleus with  $I = \frac{1}{2}$  placed in an external static magnetic field,  $B_0$ . The energy levels are given by Eq. 4 and illustrated in Fig. 1. Note that the magnetic field splits the energy levels into two non-degenerate states which are abbreviated as  $\alpha$  (the lower energy state) and  $\beta$ . The energy difference between these states is given by

$$|\Delta E| = |\gamma B_0 \hbar| = |\Omega_L \hbar| \quad (5)$$

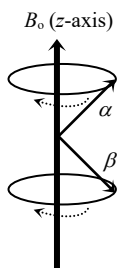
So the frequency difference between the states corresponds to the Larmor frequency. Incident electromagnetic radiation resonant with this energy difference can cause transitions between the two states. In linear units (Hz) the Larmor frequency can be expressed as:

$$\nu_L = \frac{\Omega_L}{2\pi} \quad (6)$$

Most magnets used for NMR spectroscopy produce a Larmor frequency in the radio frequency (RF) range of the electromagnetic spectrum.

Classically, the system is described as a magnetic moment rotating around the  $B_0$  vector at a rate given by the Larmor frequency where the magnetic moment is either aligned with the field ( $\alpha$ ) or against the field ( $\beta$ ), illustrated in Fig. 2. Most nuclei have a positive value for  $\gamma$ , physically meaning the magnetic moment and angular momentum point in the same direction, and therefore have a negative value for the Larmor frequency, meaning the vectors rotate clockwise around the external magnetic field.

**Figure 2.** Classical description (vector model) of a spin- $\frac{1}{2}$  nucleus in an external magnetic field. The rate of rotation about  $B_0$  is given by the Larmor frequency.



The variation in Larmor frequencies are attributed to the chemical environment of the nucleus and leads to the *chemical shift scale* used in NMR spectroscopy.

## Spin Packets, Net Magnetization, and Real Samples

In a real sample there will be many identical molecules and the nuclei will be shielded by the electrons surrounding them, so even the simple case of a molecule having a single spin of  $I = \frac{1}{2}$  requires some modification to the descriptions given above. First, as stated, the electrons will shield the nuclei from the external magnetic field, which can be described as:

$$\Omega_L = -\gamma B_0(1 - \sigma) = -\gamma B_{eff} \quad (7)$$

where  $\sigma$  is called the *shielding constant* and accounts for the effective field ( $B_{eff}$ ) each nucleus experiences.  $\sigma$  values for a given nuclide tend to vary on the order of ppm so all nuclei of a given nuclide will have very similar Larmor frequencies to each other, but generally quite different frequencies than other nuclides. For example,  $^1\text{H}$  nuclei in most small molecules exhibit Larmor frequencies that span a range of  $\sim 10$  ppm. The second modification to the descriptions given in the previous section is to group identical spins together into what are called *spin packets* and consider only their resulting *net magnetization*. For a sample at thermal equilibrium consisting of a single spin of  $I = \frac{1}{2}$  there are slightly more nuclei in the  $\alpha$  state compared to the  $\beta$  state so collectively they will produce a net magnetization aligned with the z-axis (i.e. the direction of the  $B_0$  field), as illustrated in Fig. 3. Unless otherwise specified, vector diagrams used for the rest of the handout will always be describing the net magnetization produced by a spin packet of identical spins instead of individual magnetic moments.

## Pulse Spectroscopy

If a short burst (i.e. a *pulse*) of EM radiation is applied to a sample with a frequency similar to the Larmor frequency of nuclei present, the magnetic field of the radiation will interact with those nuclei inducing transitions between the  $\alpha$  and  $\beta$  states and creating a *coherence* (a superposition of states) between them. Specifically, the selection rules for inducing a transition between states dictate that  $\Delta m = \pm 1$  so for a nucleus with  $I = \frac{1}{2}$  the transition between  $\alpha$  and  $\beta$  states is allowed. Using the vector model this can be visualized as the applied magnetic field,  $B_1$ , applying a torque to the net magnetization causing it to rotate about the negative  $B_1$  axis at a rate depending on the magnitude of the  $B_1$  field. Pulses are described by the negative axis of the  $B_1$  field and the angle through which the magnetization is rotated, which is called the *pulse angle*. This is illustrated in Figure 4, which demonstrates a “90° y-pulse” or  $\pi/2_y$  pulse rotating the net magnetization (or the double cone in Fig. 3) from the +z-axis to the +x-axis. The rotations follow the *right-hand rule*, where you place your thumb on the rotation axis (+y in this case), place your fingers in the direction of the magnetization vector (+z in this case), and then curling your fingers shows the direction of the rotation (towards +x in this case). Think about where the vector ends up in the xy-plane if an x-pulse were used instead.

**Figure 3.** Net magnetization produced by considering the vector sum of all identical nuclei in a sample. Note that the net magnetization is stationary in this picture even though the individual spins are rotating about the z-axis at the Larmor frequency.

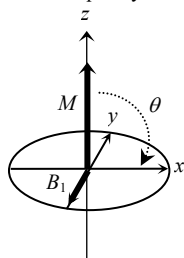
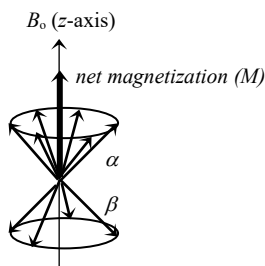


**Figure 4.** Response of the net magnetization to a pulse of EM radiation ( $B_1$ ).

When the magnetization is rotated into the  $xy$ -plane it also precesses about the  $+z$ -axis at the Larmor frequency. However, to simplify descriptions vector diagrams generally use a *rotating frame* model where the entire  $xy$ -plane rotates about the  $+z$ -axis at a given frequency. For reasons that will be made clear later, the reference frequency for the rotating frame is chosen to be the frequency of the  $B_1$  field. In this rotating frame the net magnetization precesses in the  $xy$ -plane at a frequency that corresponds to the *difference* between the Larmor frequency and the frequency of the  $B_1$  field.

After the application of a pulse the system responds by moving back towards its thermal equilibrium state (as shown in Fig. 3). This is described in terms of two separate effects: 1) reestablishing the thermal equilibrium populations of the  $\alpha$  and  $\beta$  states, and 2) the loss of coherence between the two states. The former process is called spin-lattice relaxation and is given a time constant  $T_1$ . The latter process is called spin-spin relaxation and is given a time constant  $T_2$ .

For NMR spectroscopy a coil of wire is set up in an orientation such that magnetization precessing in the  $xy$ -plane induces a current in the coil. The induced current is then measured over time producing a signal called the *free induction decay* (FID). The simplest NMR experiment consists of a pulse to put the net magnetization into the  $xy$ -plane followed by measurement of the FID, shown schematically in Fig. 5. As part of the signal conditioning the frequency of the applied pulse (called the *carrier frequency*) is subtracted from the frequency components of the net magnetization before digitization so the FID contains the frequency difference. A Fourier transform (FT) is then used to convert the time domain FID into the frequency domain where the various frequency components of the magnetization can be analyzed. Below is an example of a signal with a Larmor frequency  $+10$  Hz relative to the reference frequency (i.e.  $\Delta = +10$  Hz):

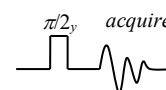


**Figure 5.** The simplest NMR experiment is a pulse followed by acquisition of the FID, shown above.

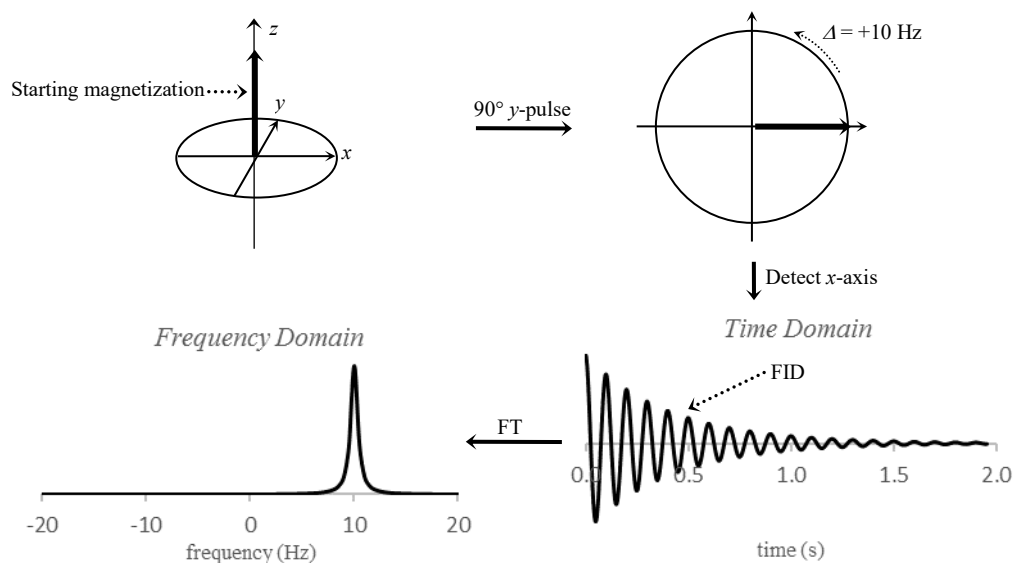


**Figure 6.** Acquisition of data from the experiment shown in Fig. 5. The magnetization starts at thermal equilibrium on the  $z$ -axis (upper-left). The pulse moves the net magnetization to the  $x$ -axis where it rotates  $+10$  Hz relative to the reference frequency (upper-right). The rotating magnetic moment induces a current in a coil of wire that is positioned to record the  $x$ -component of the magnetization (lower-right). The signal decays as the magnetization returns to the  $+z$ -axis. A Fourier transform converts the time domain signal into the frequency domain (lower-right).

In the case where many chemically distinct nuclei of the same nuclide are in the sample, they will all rotate in the  $xy$ -plane with their corresponding Larmor frequencies. The FID contains the sum of all the individual components. The FT extracts all the frequency components in the pattern, as shown below:

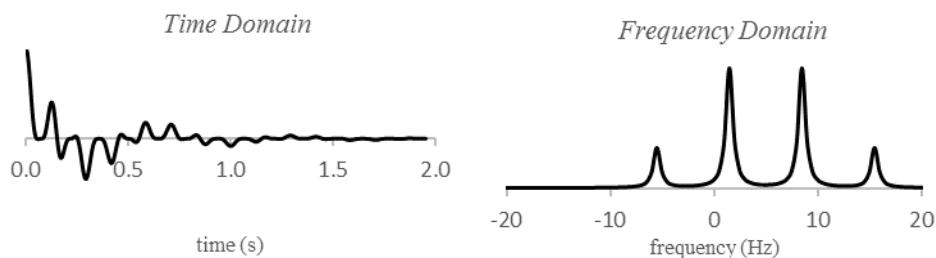


**Figure 7.** FID with many individual components (left) and its Fourier transform (right).

In an actual molecule there are generally even more signals. Below is a  $^1\text{H}$  spectrum of 3-heptanone:

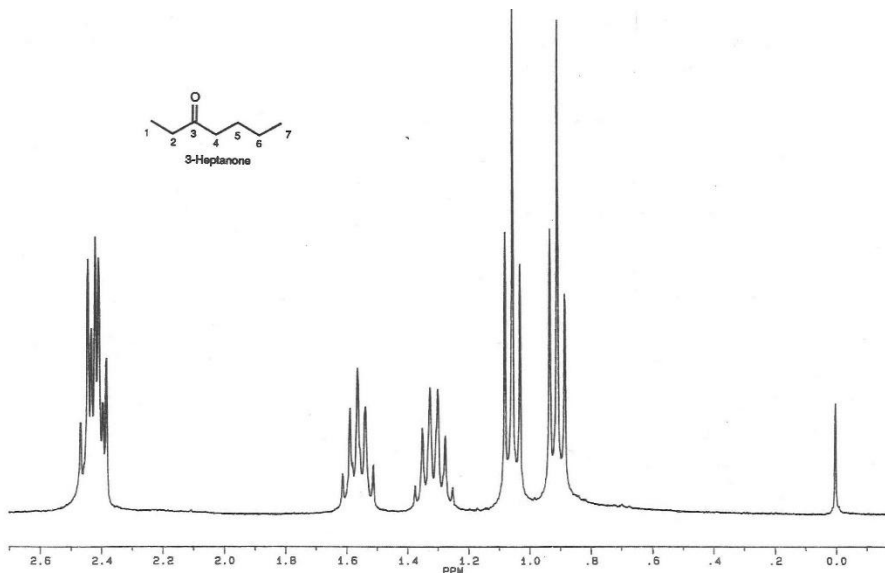


**Figure 8.**  $^1\text{H}$  spectrum of 3-heptanone.  $J$ -coupling and chemical shift data allow for most assignments to be made but the two methyl groups cannot be assigned conclusively.

### Lineshapes

A Lorentzian lineshape is observed in NMR spectroscopy, which has two different forms: an *absorption mode* form that has a non-zero integrated intensity and a *dispersion mode* form that has zero integrated intensity. The position of the magnetization in the  $xy$ -plane at the start of acquisition determines the specific lineshape observed in the spectrum. By convention, if the magnetization is on the  $x$ -axis then an absorptive lineshape is observed and if it is on the  $y$ -axis then a dispersive lineshape is observed. This is illustrated below in Fig. 9.

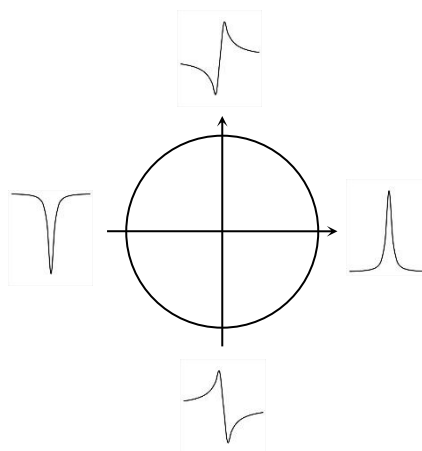
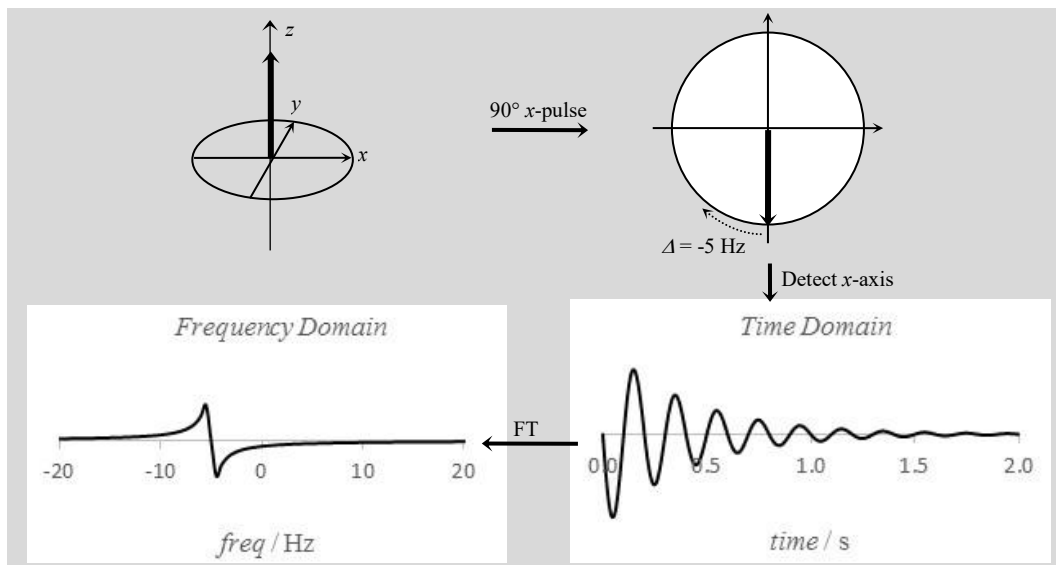


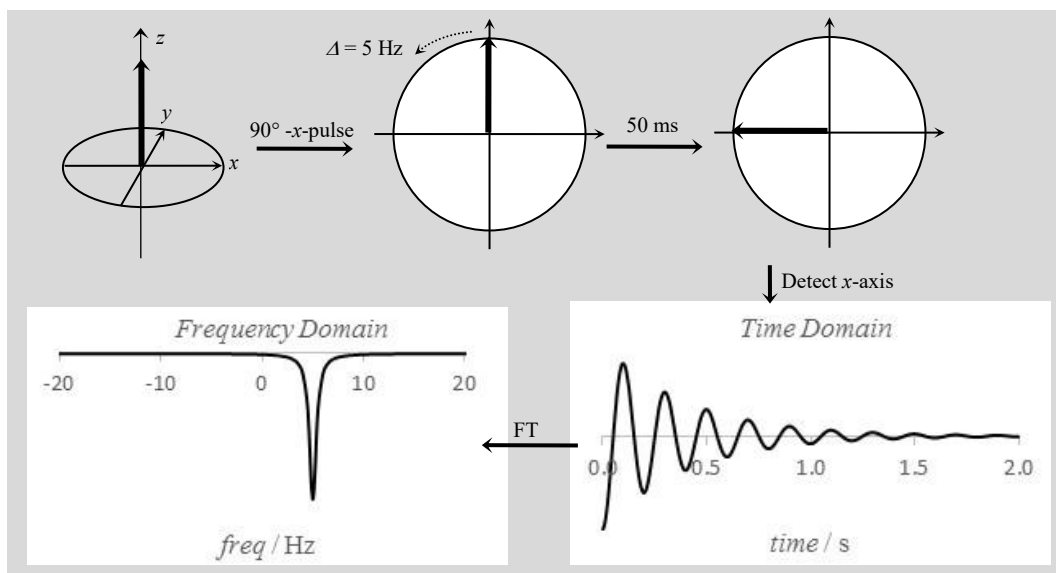
**Figure 9.** The observed lineshape depends on the position of the magnetization vector at the start of acquisition: absorptive lineshapes are observed when the magnetization is on the  $x$ -axis and dispersive lineshapes are observed when the magnetization is on the  $y$ -axis. If the magnetization is between axes then a mixture of the lineshapes is observed.

In practice there is always some ambiguity about the absolute position of the magnetization at the start of acquisition, resulting in a *phase error* in the acquired spectrum. This means all spectra appear initially with signals as a mixture of the two forms, but this can be corrected mathematically, which the processing software performs in a process called *phasing*. Note that although this means the absolute phase of a signal is arbitrary, the relative phase between different signals in a spectrum is fixed.

**Self Check #1:** Repeat the analysis given in Fig. 6 using an x-pulse instead of the y-pulse and  $\Delta = -5$  Hz.



**Self Check #2:** Repeat the analysis given in Fig. 6 using a -x-pulse,  $\Delta = 5$  Hz, and add a delay of 50 ms before the acquisition.



### System of Coupled Spins of $I = \frac{1}{2}$

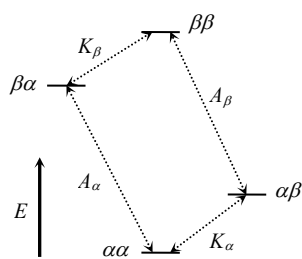


**Figure 10.** Energy levels for an  $AK$  system of spins of  $\frac{1}{2}$  showing all possible transitions from a single pulse.

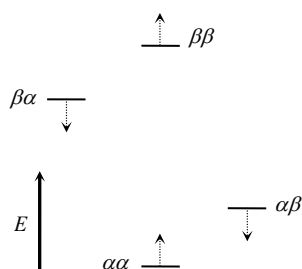


**Figure 11.** Change in the energy levels due to  $J$ -coupling. Note that each energy level is shifted by  $J/4$  Hz in the direction shown.

One of the key types of information that NMR spectroscopy provides is the chemical shift, which is due to the shielding caused by its local environment. This information can help to identify functional groups present in the molecule. For example, in Fig. 8 the carbonyl group attracts electron density away from the nuclei around it so  $^1\text{H}$  nuclei near it appear with a larger chemical shift (less shielded by neighboring electrons). You can also see in the figure that each overall signal appears to exhibit splitting into a multiplet. This splitting is due to interactions with neighboring nuclei, called spin-spin (or  $J$ ) coupling.

Consider a simple system of only two  $I = \frac{1}{2}$  spins of different nuclides, called  $A$  and  $K$ . Since each nucleus can be in one of two possible states ( $\alpha$  or  $\beta$ ), there are four states total:  $\alpha\alpha$ ,  $\alpha\beta$ ,  $\beta\alpha$ , and  $\beta\beta$ , where the first letter gives the spin state of the  $A$  nucleus and the second letter gives the spin state of the  $K$  nucleus. The energy of each state is simply the sum of the Zeeman interaction for each nucleus, as given in Eq. 8 and shown in Fig. 10. Expressing this in frequency units in the rotating frame

$$E_{AK}/h = -\gamma_A B_0 m_A - \gamma_K B_0 m_K = \Omega_A m_A + \Omega_K m_K \quad (8)$$

Remember that the selection rules require  $\Delta m = 1$  for a transition, so in this case it means one of the two nuclei can change states upon interacting with the applied field. The allowed transitions are shown in the figure. Since only one nucleus can change state at a time, the transitions are labeled with the nucleus that is changing states, so  $\alpha\alpha \rightarrow \alpha\beta$  is a “ $K$ ” transition since the  $K$  nucleus changes state. More specifically, the transition is labeled as “ $K_\alpha$ ” since the  $A$  nucleus is in the  $\alpha$  state throughout the transition. Take time to familiarize yourself with the naming convention for each transition in the figure. Note that in Fig. 10, the  $A_\alpha$  and  $A_\beta$  transitions are degenerate, as well as the  $K_\alpha$  and  $K_\beta$  transitions.

If the two nuclei can interact with each other (e.g. through the bonding electrons that connect them) then these energy levels are perturbed by a slight amount and Eq. 8 is modified to

$$E_{AK}/h = \Omega_A m_A + \Omega_K m_K + 2\pi J m_A m_K \quad (9)$$

where  $J$  is the scalar coupling constant in units of Hz. Figure 11 illustrates the perturbations of the energy level assuming the value for  $J$  is positive. Note from the figure that in the absence of coupling the two transitions of the  $K$  nucleus are degenerate as well as the two transitions for the  $A$  nucleus, but in the presence of spin-spin coupling the  $K_\beta$  transition (flipping the spin of  $K$  while the  $A$  nucleus is in the  $\beta$  state) is perturbed to higher energy and the  $K_\alpha$  transition is perturbed to lower energy; the  $A$  transitions are perturbed in a similar fashion. Since the  $m$  values are  $\frac{1}{2}$  or  $-\frac{1}{2}$ , each energy level is displaced by  $J/4$  Hz. This means, for example, that the  $K_\beta$  transition is displaced by  $J/2$  Hz to larger (more negative) frequency, and the  $K_\alpha$  transition is displaced by  $J/2$  Hz to smaller (less negative frequency). The frequency difference between  $K_\alpha$  and  $K_\beta$  is  $J$  Hz. The corresponding vector diagrams for the evolution of the two  $K$  transitions from the  $+x$ -axis are shown below.

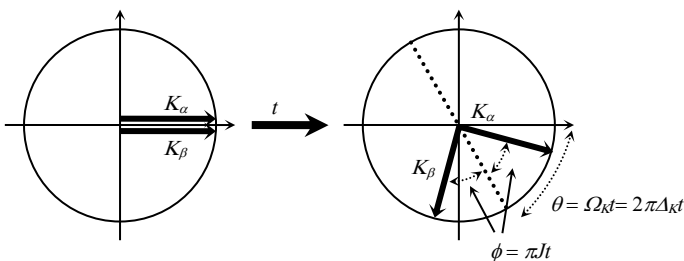


**Figure 12.** Evolution of the coherences for the two  $K$  transitions starting on the  $+x$ -axis after a time,  $t$ . Note that the frequency of the  $K_\alpha$  transition is  $\Delta_K + J/2$  Hz and the frequency of the  $K_\beta$  transition is  $\Delta_K - J/2$ .  $\Delta_K$  is a negative value as shown but could be any value. Also note that by convention  $\Delta$  is expressed in linear units (Hz); in angular units the symbol  $\Omega$  is used instead.

Spin-spin coupling extends well beyond the simple case of two spins. For example, a  $\text{CH}_3\text{CH}_2-$  fragment will have the signal for the methyl group split into a 1:2:1 triplet and the signal for the methylene will be split into a 1:3:3:1 quartet (consider the possible spin states for the neighboring nuclei, and see Fig. 13). This information is often critical for identifying connectivity in a molecule, as well as *cis/trans* conformation, and so forth.

**Self Check #3:** Repeat the analysis given in Fig. 6 for the system of coupled nuclei ( $AK$ ) just described, but with the following modifications: 1) the pulse is only resonant with the  $A$  transitions (won't affect the  $K$  transitions), 2)  $\Delta_A = 5$  Hz, 3)  $J = 30$  Hz, and 4) ignore sketching the time domain signal.

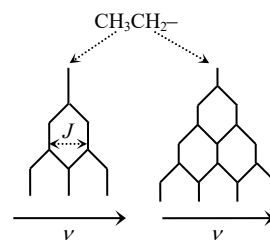
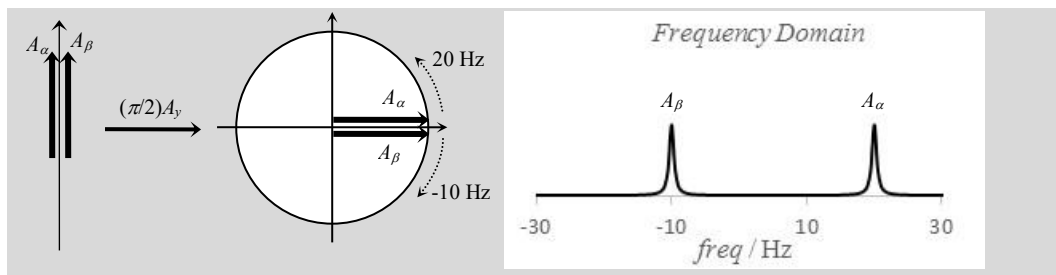
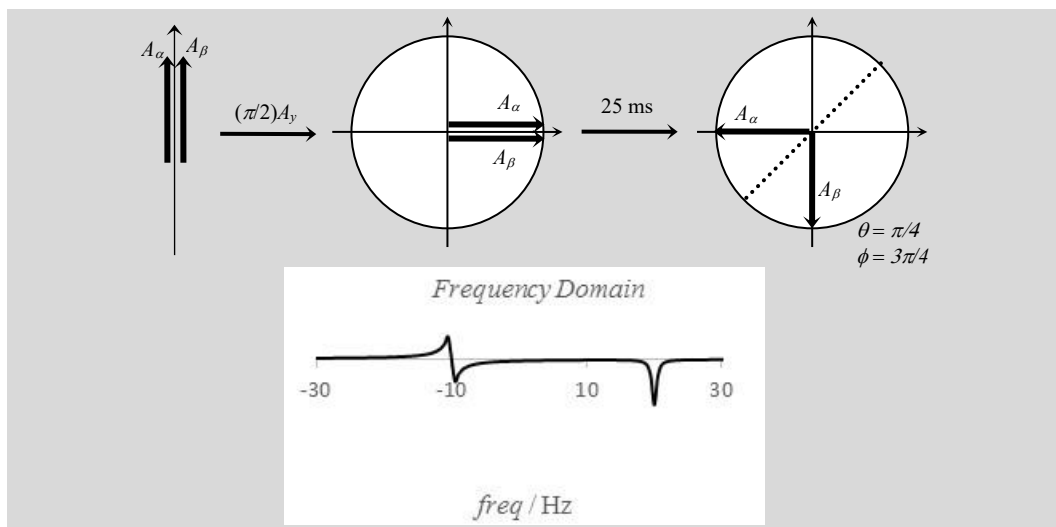


**Figure 13.** Splitting of a methyl signal by a methylene group producing a triplet, and splitting of a methylene group by a methyl group producing a quartet. Note that the spacing of each split is identical.

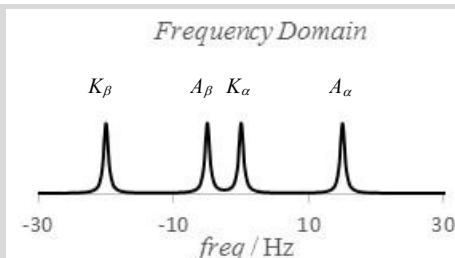


**Self Check #4:** Repeat the process above but add a delay of 25 ms before the acquisition.



**Self Check #5:** Repeat **Self Check #3**, but with the following modifications: 1)  $A$  and  $K$  are the same nuclide so the pulse is resonant with both the  $A$  and  $K$  transitions and both sets of transitions are in the same reference frame, 2)  $\Delta_A = 5$  Hz, 3)  $\Delta_K = -10$  Hz, and 4)  $J = 20$  Hz.

The pulse puts all four vectors on the  $+x$ -axis so they all have a positive absorptive line shape. The frequencies are  $5 \pm 10$  Hz for the  $A$  vectors, and  $-10 \pm 10$  Hz for the  $K$  vectors.



## Theory – Quantum Mechanical Description

### Basic Principles

Visualizing the net magnetization as a vector in physical space is the *classical description* of NMR. This description is easy to grasp and it does make correct predictions of the observed spectra for the cases discussed so far. However, it fails to correctly predict the behavior of the system and

the observed spectra in most experiments involving multiple pulses and coupled nuclei. To correctly predict the results of experiments, a *quantum mechanical description* of NMR is required. Quantum mechanical treatments can be substantially more difficult to grasp, so presented here is only a partial description. A full mathematical description is not required to perform the operations and understand NMR experiments.

To start, recall in quantum mechanics the state of any system can be described by a wave function,  $|\psi\rangle$ . The wave functions of particular interest in spectroscopy are those that are eigenfunctions of the Hamiltonian (energy) operator, represented by the time-independent Schrödinger equation,  $H|\psi\rangle = E|\psi\rangle$ . In NMR, the set of wave functions that are eigenfunctions of the Hamiltonian operator are specified by the two quantum numbers,  $I$  and  $m_I$ , as  $|I, m_I\rangle$ . The exact expression of the wave function is not necessary, only specification of the quantum numbers is needed. Furthermore, since  $I$  is known for any given nucleus, the wave functions can be simplified even further by simply specifying  $m_I$ . Thus, for a nucleus with  $I = 1/2$  the two wave functions that are eigenfunctions of the Hamiltonian operator are  $|1/2\rangle$  and  $|-1/2\rangle$ . Also, as discussed earlier, since there are only two states we generally refer to them as simply  $\alpha$  and  $\beta$ , respectively. These wave functions form an orthonormal basis set meaning  $\langle i | j \rangle = 1$  if  $i = j$  and  $\langle i | j \rangle = 0$  if  $i \neq j$ . They are also eigenfunctions of the operator for the  $z$ -component of the magnetization,  $I_z$ :

$$I_z |m_I\rangle = m_I |m_I\rangle \quad (10)$$

Now let's revisit some of the equations from before from a quantum mechanical approach. Recall that the energy of the interaction of a magnetic dipole ( $\mu$ ) in an external magnetic field ( $B_0$ ) is given by  $E = -\mu \cdot B_0$ . With the direction of the external magnetic field taken to be the  $z$ -axis, we can write the Hamiltonian operator as  $H = -\mu_z B_0 = -\gamma B_0 I_z = \Omega_L I_z$ . You should recognize the  $-\gamma B_0$  term as the Larmor frequency expressed in angular units,  $\Omega_L$ . Solving the time-independent Schrödinger equation then follows as:

$$\begin{aligned} H|\psi\rangle &= E|\psi\rangle \\ \Omega_L I_z |\alpha\rangle &= \Omega_L (1/2) |\alpha\rangle \quad \Omega_L I_z |\beta\rangle = \Omega_L (-1/2) |\beta\rangle \end{aligned} \quad (11)$$

This, of course, is the same result presented earlier (Eq. 5): two states with a difference corresponding to the Larmor frequency of the nucleus.

For the case of two coupled spins,  $A$  and  $K$ , the basis set is expanded to four terms with the wave functions specified by the two  $m_I$  values, which are specified as  $m_A$  and  $m_K$ . Instead of specifying the angular momentum operators as  $I_{Az}$ , we will also abbreviate the notation and simply use  $A_z$  instead (the  $I$  being implied). The same eigenvalue equations apply as before, so

$$A_z |m_A, m_K\rangle = m_A |m_A, m_K\rangle \quad K_z |m_A, m_K\rangle = m_K |m_A, m_K\rangle \quad (12)$$

The Hamiltonian operator consists of the two Zeeman interactions and the coupling between the two nuclei. In the rotating frame, the Hamiltonian is written as:

$$H = \Omega_A A_z + \Omega_K K_z + 2\pi J A_z K_z \quad (13)$$

You should see the similarities between this and Eq. 9, noting that the  $z$ -operators return the corresponding  $m$  value.

### Matrix Form of Operators

It is beneficial to express the angular momentum operators in a matrix format, both for visualization and for performing the mathematical operations. To do this the kets are represented in the columns and the bras are represented in the rows. So for a nucleus with  $I = 1/2$  where there are just two basis functions  $|\alpha\rangle$  and  $|\beta\rangle$ , any operator  $O$  can be written as

$$O = \begin{pmatrix} \langle \alpha | O | \alpha \rangle & \langle \alpha | O | \beta \rangle \\ \langle \beta | O | \alpha \rangle & \langle \beta | O | \beta \rangle \end{pmatrix} \quad (14)$$



Since  $|\alpha\rangle$  and  $|\beta\rangle$  are eigenfunctions of  $I_z$  and are orthonormal, it is relatively straightforward to write the matrix form of  $I_z$ :

$$I_z = \begin{pmatrix} \langle \alpha | I_z | \alpha \rangle & \langle \alpha | I_z | \beta \rangle \\ \langle \beta | I_z | \alpha \rangle & \langle \beta | I_z | \beta \rangle \end{pmatrix} = \begin{pmatrix} 1/2 \langle \alpha | \alpha \rangle & -1/2 \langle \alpha | \beta \rangle \\ 1/2 \langle \beta | \alpha \rangle & -1/2 \langle \beta | \beta \rangle \end{pmatrix} = \frac{1}{2} \begin{pmatrix} 1 & 0 \\ 0 & -1 \end{pmatrix}$$

$|\alpha\rangle$  and  $|\beta\rangle$  are not eigenfunctions of the  $I_x$  and  $I_y$  operators, but their derivation follows a similar process and you will work them out in one of the daily activities. For now, we'll just accept the following definitions:

$$I_x = \frac{1}{2} \begin{pmatrix} 0 & 1 \\ 1 & 0 \end{pmatrix} \quad I_y = \frac{1}{2} \begin{pmatrix} 0 & -i \\ i & 0 \end{pmatrix} \quad I_z = \frac{1}{2} \begin{pmatrix} 1 & 0 \\ 0 & -1 \end{pmatrix} \quad (15)$$

For the case of two spins, these single-spin operators must be combined to produce the corresponding two-spin operators using an operation called the direct product,  $\otimes$ . The overall format is  $I_i \otimes I_j$  where  $I_i$  is one of the angular momentum operators, or the identity matrix ( $I$ ), to represent the  $A$  nucleus and  $I_j$  is one of the angular momentum operators, or the identity matrix, to represent the  $K$  nucleus. Since there are four possibilities each for  $I_i$  and  $I_j$  there are 16 total two-spin angular momentum operators. The direct product is calculated as

$$\begin{pmatrix} a & b \\ c & d \end{pmatrix} \otimes \begin{pmatrix} e & f \\ g & h \end{pmatrix} = \begin{pmatrix} a \begin{pmatrix} e & f \\ g & h \end{pmatrix} & b \begin{pmatrix} e & f \\ g & h \end{pmatrix} \\ c \begin{pmatrix} e & f \\ g & h \end{pmatrix} & d \begin{pmatrix} e & f \\ g & h \end{pmatrix} \end{pmatrix} = \begin{pmatrix} ae & af & be & bf \\ ag & ah & bg & bh \\ ce & cf & de & df \\ cg & ch & dg & dh \end{pmatrix} \quad (16)$$

For labelling the operators, the  $I$  is dropped so a term that would formally be  $I_{Ax}$ , for example, is written as simply  $A_x$ . With this notation, the  $A_x$  operator for the two-spin case is given below:

$$I_x \otimes \mathbf{1} = \frac{1}{2} \begin{pmatrix} 0 & 1 \\ 1 & 0 \end{pmatrix} \otimes \begin{pmatrix} 1 & 0 \\ 0 & 1 \end{pmatrix} = \frac{1}{2} \begin{pmatrix} 0 & 0 & 1 & 0 \\ 0 & 0 & 0 & 1 \\ 1 & 0 & 0 & 0 \\ 0 & 1 & 0 & 0 \end{pmatrix} = "A_x" \quad (17)$$

Compare this to the  $K_x$  operator derived as:

$$\mathbf{1} \otimes I_x = \begin{pmatrix} 1 & 0 \\ 0 & 1 \end{pmatrix} \otimes \frac{1}{2} \begin{pmatrix} 0 & 1 \\ 1 & 0 \end{pmatrix} = \frac{1}{2} \begin{pmatrix} 0 & 1 & 0 & 0 \\ 1 & 0 & 0 & 0 \\ 0 & 0 & 0 & 1 \\ 0 & 0 & 1 & 0 \end{pmatrix} = "K_x" \quad (18)$$

How do these operators relate to the classical vector diagrams discussed earlier in the handout? Or phrased another way, how do we visualize these operators? The key is to relate the operator to the energy level diagram given in Fig. 10. Let's write the  $A_x$  operator in a more symbolic way, labelling the rows and columns with the corresponding states:

	$\alpha\alpha$	$\alpha\beta$	$\beta\alpha$	$\beta\beta$
$\alpha\alpha$	0	0	1	0
$\alpha\beta$	0	0	0	1
$\beta\alpha$	1	0	0	0
$\beta\beta$	0	1	0	0

In this form, you can see there are coefficients of 1 in locations that connect states  $\beta\alpha$  and  $\alpha\alpha$  together, as well as states  $\alpha\beta$  and  $\beta\beta$  together. In Fig. 10 these connections represent the  $A_\alpha$  and  $A_\beta$  transitions, respectively. Since the coefficients in the matrix are complex numbers, the typical mathematical convention is used where the real component is represented on the x-axis and the imaginary component is represented on the y-axis. Therefore, the  $A_x$  operator has a vector

representation where both the  $A_\alpha$  and  $A_\beta$  vectors are together on the  $+x$ -axis, as shown in Fig. 14. Using this logic an “interpretive form” of the operators can be written, as shown below:

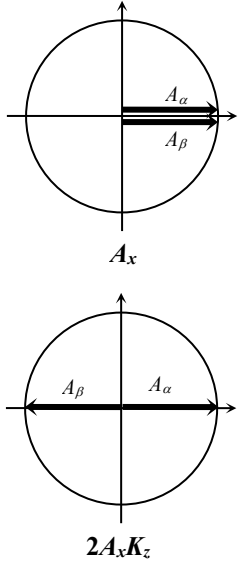


**Figure 14.** Vector diagrams of  $A_x$  and  $2A_x K_z$ .

$$\begin{pmatrix} P_{\alpha\alpha} & K_\alpha^* & A_\alpha^* & DQ^* \\ K_\alpha & P_{\alpha\beta} & ZQ^* & A_\beta^* \\ A_\alpha & ZQ & P_{\beta\alpha} & K_\beta^* \\ DQ & A_\beta & K_\beta & P_{\beta\beta} \end{pmatrix} \quad (19)$$

With this interpretive form a set of two vector diagrams, one for each rotating reference frame, can be sketched to represent the matrix in a classical form. The details of creating such a picture have been discussed in the text above, and summarized in the table below:

Vector	$x$	$y$	$z$
$A_\alpha$	$2*Re(A_\alpha)$	$2*Im(A_\alpha)$	$P_{\alpha\alpha} - P_{\beta\alpha}$
$A_\beta$	$2*Re(A_\beta)$	$2*Im(A_\beta)$	$P_{\alpha\beta} - P_{\beta\beta}$
$K_\alpha$	$2*Re(K_\alpha)$	$2*Im(K_\alpha)$	$P_{\alpha\alpha} - P_{\alpha\beta}$
$K_\beta$	$2*Re(K_\beta)$	$2*Im(K_\beta)$	$P_{\beta\alpha} - P_{\beta\beta}$

**Table 1.** Relationships between the two-spin density matrix defined in Eq. 19 and the  $x$ -,  $y$ -, and  $z$ -components of classical vector diagrams for the four transitions allowed in NMR spectroscopy. The functions  $Re(w)$  and  $Im(w)$ , return the real and imaginary components, respectively of  $w$ .

Because the matrix is Hermitian (element  $ij$  is the complex conjugate of element  $ji$ ) we only need to focus on the lower-left triangle of the matrix. The diagonal terms represent relative populations of the stationary states and their differences correspond to the  $z$ -components of the magnetization. Recall from the double-cone picture in Fig. 3 that the net  $z$ -component is the difference in population between the  $\alpha$  and  $\beta$  states ( $P_\alpha - P_\beta$ ). In the two-spin system there are 4 classical vectors so the  $z$ -component of the  $A_\alpha$  vector, for example, is calculated as  $P_{\alpha\alpha} - P_{\beta\alpha}$ . The off-diagonal terms represent a coherent superposition (*coherence*) between two states and are represented classically with the  $x$ - and  $y$ -components of the magnetization, as described previously. The  $ZQ$  and  $DQ$  terms (called zero-quantum and double-quantum, respectively) represent coherences for the  $\alpha\alpha \leftrightarrow \beta\beta$  and  $\beta\alpha \leftrightarrow \alpha\beta$  transitions. These terms do not have a classical representation in either the  $A$  or  $K$  rotating reference frame since their rotational frequencies do not correspond to the frequencies of either the  $A$  or  $K$  transitions.

Note that in Fig. 12, the  $J$ -coupling causes the two transitions to dephase relative to each other, but there is no such dephasing present in either the  $A_x$  or  $A_y$  operators (or in the  $K_x$  or  $K_y$  operators). So how is the dephasing represented in the basis operators? The answer is in some of the operators not yet examined. Consider the following combination:

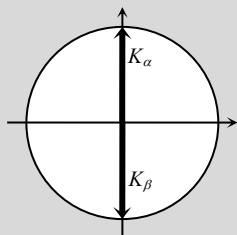
$$2(I_x \otimes I_z) = 2 \left( \frac{1}{2} \begin{pmatrix} 0 & 1 \\ 1 & 0 \end{pmatrix} \otimes \frac{1}{2} \begin{pmatrix} 1 & 0 \\ 0 & -1 \end{pmatrix} \right) = \frac{1}{2} \begin{pmatrix} 0 & 0 & 1 & 0 \\ 0 & 0 & 0 & -1 \\ 1 & 0 & 0 & 0 \\ 0 & -1 & 0 & 0 \end{pmatrix} = "2A_x K_z" \quad (20)$$

The multiplication by 2 is required for normalization so the basis operators are all the same size. Note that both the  $2A_x K_z$  operator and the  $A_x$  operator have real coefficients for both the  $A_\alpha$  and  $A_\beta$  transitions but the coefficient for  $A_\beta$  is negative in the  $2A_x K_z$  operator, meaning it is on the  $-x$ -axis instead of in-phase with the  $A_\alpha$  coefficient on the  $+x$ -axis. Therefore,  $2A_x K_z$  is called an *antiphase operator*, whereas  $A_x$  is an *in-phase operator*.

The operators that have classical vector representations (such as those shown in Fig. 14) are  $A_x$ ,  $A_y$ ,  $A_z$ ,  $K_x$ ,  $K_y$ ,  $K_z$ ,  $2A_x K_z$ ,  $2A_y K_z$ ,  $2A_z K_x$ ,  $2A_z K_y$ , and  $2A_z K_z$ . The remaining operators ( $2A_x K_x$ ,  $2A_x K_y$ ,  $2A_y K_x$ , and  $2A_y K_y$ ) represent the  $ZQ$  and  $DQ$  transitions and do not have classical vector representations.

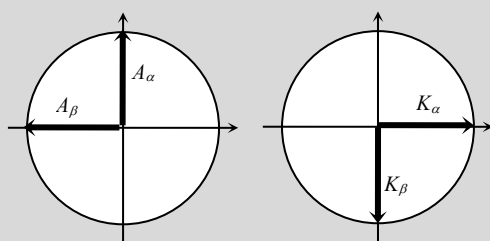
**Self Check #6:** Calculate the matrix for the  $2A_zK_y$  basis operator and sketch the corresponding vector diagram(s).

$$2(I_z \otimes I_y) = 2 \left( \frac{1}{2} \begin{pmatrix} 1 & 0 \\ 0 & -1 \end{pmatrix} \otimes \frac{1}{2} \begin{pmatrix} 0 & -i \\ i & 0 \end{pmatrix} \right) = \frac{1}{2} \begin{pmatrix} 0 & -i & 0 & 0 \\ i & 0 & 0 & 0 \\ 0 & 0 & 0 & i \\ 0 & 0 & -i & 0 \end{pmatrix}$$



**Self Check #7:** Sketch the corresponding vector diagram(s) for the following matrix:

$$\frac{1}{2} \begin{pmatrix} 0 & 1 & -i & 0 \\ 1 & 0 & 0 & -1 \\ i & 0 & 0 & i \\ 0 & -1 & -i & 0 \end{pmatrix}$$



Note that, in general, the  $A$  and  $K$  vectors are in separate rotating frames.

### Product Operator Formalism

The state of any arbitrary system, given by a similar matrix called the *density matrix*, can be represented as a linear combination of the angular momentum operators, called a *basis set expansion*. This is analogous to expressing the location of a point in space using Cartesian coordinates. With this representation, the effects of pulses and delays can be performed as classical vector rotations (instead of raw matrix multiplications) leading to a simple algorithmic approach to applying quantum mechanics in NMR, called the *product operator formalism*. By convention, these rotations follow the *right-hand rule* where your thumb is placed in the direction of the rotation vector and your fingers curl in the direction of a positive rotation. Using this convention, the following orders are defined for the Cartesian coordinate system (see Fig. 15):

$$\begin{aligned} z\text{-axis: } & x \rightarrow y \rightarrow -x \rightarrow -y \\ x\text{-axis: } & y \rightarrow z \rightarrow -y \rightarrow -z \\ y\text{-axis: } & z \rightarrow x \rightarrow -z \rightarrow -x \end{aligned}$$

These orders are cyclical so the last term given above in each sequence cycles back to the beginning. Calculation of the position of a vector after a rotation of  $\theta$  radians around an arbitrary basis vector,  $V_{rot}$ , follows basic trigonometry:

$$V_{start} \xrightarrow{\theta V_{rot}} V_{start} \cos(\theta) + V_{next} \sin(\theta) \quad (21)$$

where  $V_{start}$  is the starting basis vector, and  $V_{next}$  is the basis vector after a  $+90^\circ$  rotation. For example, rotating a unit vector starting on the  $x$ -axis by  $\theta$  radians around the  $z$ -axis is written as:  $x \xrightarrow{\theta z} x \cos \theta + y \sin \theta$ . In NMR we use the angular momentum basis set, but many of the relationships between the various angular momentum operators can be visualized analogous to the Cartesian system. Some example relationships are shown below:

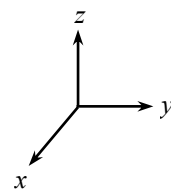
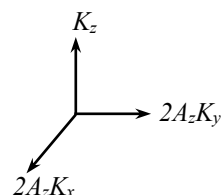
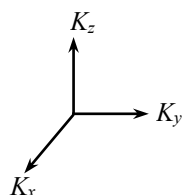
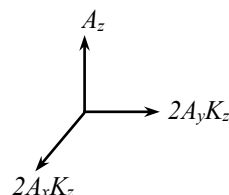
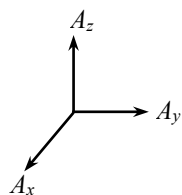


**Figure 15.** The  $xyz$  Cartesian coordinate system (the  $x$ -axis is coming out of the page). For rotations, place your thumb along the axis to be rotated and your fingers curl in the direction of a positive rotation.



You will explore these relationships further in the written activities, and learn how to derive them from classical vector pictures of the basis operators. Given these relationships, some example rotations are shown below:

$$A_x \xrightarrow{\theta A_z} A_x \cos \theta + A_y \sin \theta$$

$$A_z \xrightarrow{\theta A_y} A_z \cos \theta + A_x \sin \theta$$

$$A_y \xrightarrow{\theta A_z} A_y \cos \theta - A_x \sin \theta$$

$$-2A_yK_z \xrightarrow{\theta A_z} -2A_yK_z \cos \theta + 2A_xK_z \sin \theta$$

$$K_y \xrightarrow{\theta K_x} K_y \cos \theta + K_z \sin \theta$$

$$-2A_zK_x \xrightarrow{\theta K_z} -2A_zK_x \cos \theta - 2A_zK_y \sin \theta$$

Make sure you understand each of these examples. Ask questions!

All the examples above illustrate rotation by an arbitrary angle,  $\theta$ . In NMR spectroscopy it is common for  $\theta$  to be a known, fixed angle that is a multiple of  $90^\circ$ . In these situations, one of the cos/sin terms is  $\pm 1$  and the other is 0 which allows it to be eliminated, as shown in the examples below:

$$A_z \xrightarrow{\left(\frac{\pi}{2}\right) A_y} A_x$$

$$A_y \xrightarrow{\pi A_x} -A_y$$

$$-K_x \xrightarrow{\left(\frac{\pi}{2}\right) K_z} -K_y$$

Rotating a vector around the axis it lies on does not change its position, as shown in the following examples:

$$A_x \xrightarrow{\left(\frac{\pi}{2}\right) A_x} A_x$$

$$2A_yK_z \xrightarrow{\pi A_y} 2A_yK_z$$

$$K_y \xrightarrow{\left(\frac{\pi}{2}\right) K_y} K_y$$

When performing the rotations, note that  $A$  operators only affect  $A$  terms and  $K$  operators only affect  $K$  terms. This is illustrated in the example rotations below:

$$A_x \xrightarrow{\theta K_z} A_x$$

$$2A_zK_x \xrightarrow{\pi A_x} -2A_zK_x$$

$$2A_xK_z \xrightarrow{\left(\frac{\pi}{2}\right) K_y} 2A_xK_x$$

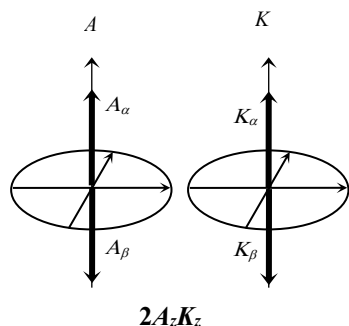
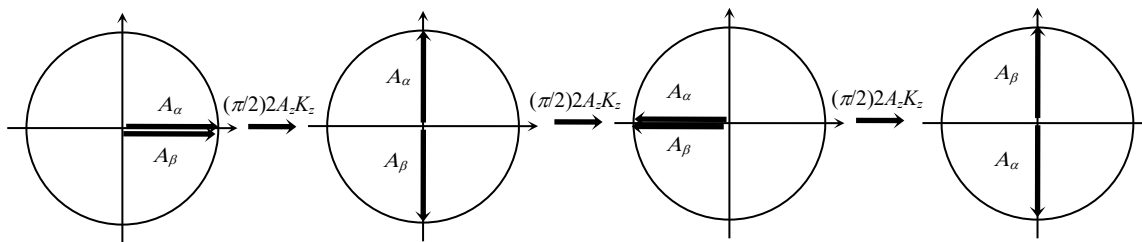


**Figure 16.** Classical vector representation of the  $2A_zK_z$  operator.

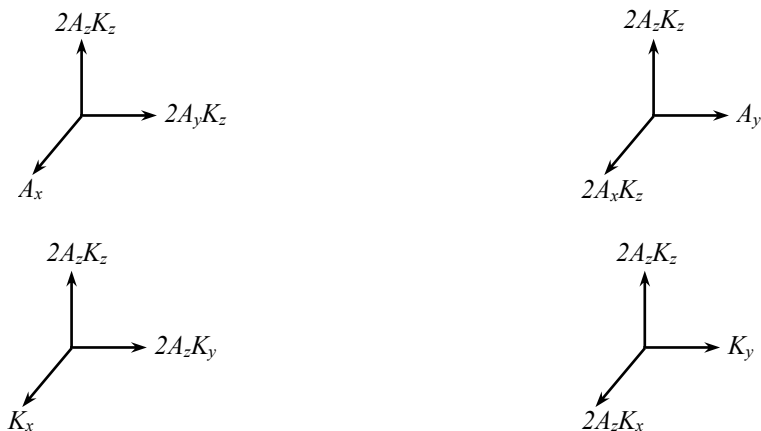
The rotations given so far model the effects of the Zeeman interaction (i.e. chemical shift) and pulses in NMR spectroscopy. Pulses are modeled as rotations around the  $x$ - or  $y$ -axis and the chemical shift is modeled as a rotation around the  $z$ -axis (the direction of the external magnetic field). The effects of  $J$ -coupling (3<sup>rd</sup> term in Eq. 15) are modeled with a slightly different rotation. Recall that  $J$ -coupling causes the  $\alpha$ -vector to rotate around the  $+z$ -axis and the  $\beta$ -vector to rotate around the  $-z$ -axis (see Fig. 12). This motion corresponds to a rotation around the  $2A_zK_z$  operator, which has a classical vector representation given in Fig. 16. Consider starting from  $A_x$  and rotate in  $90^\circ$  increments with the  $2A_zK_z$  operator (i.e. rotate the  $\alpha$ -vector in the positive direction and the  $\beta$ -vector in the negative direction). The sequence is shown below:



Note that this corresponds to the rotation cycle given below:

$$A_x \rightarrow 2A_yK_z \rightarrow -A_x \rightarrow -2A_yK_z \rightarrow A_x$$

Similar cycles can be derived starting from  $A_y$ ,  $K_x$ , and  $K_y$ , which lead to the following relationships:



**Self Check #8:** Perform the following rotations:

$$\begin{array}{lll} A_x \xrightarrow{\theta A_y} & K_y \xrightarrow{\theta A_z} & K_y \xrightarrow{\left(\frac{\pi}{2}\right) K_y} \\ 2A_zK_x \xrightarrow{\left(\frac{\pi}{2}\right) A_z} & 2A_zK_x \xrightarrow{\left(\frac{\pi}{2}\right) K_y} & 2A_xK_y \xrightarrow{\left(\frac{\pi}{2}\right) K_z} \\ 2A_yK_z \xrightarrow{\left(\frac{\pi}{2}\right) A_z} & 2A_yK_z \xrightarrow{\left(\frac{\pi}{2}\right) 2A_zK_z} & -K_x \xrightarrow{\phi 2A_zK_z} \end{array}$$

**Answers**

$$\begin{array}{lll} A_x \xrightarrow{\theta A_y} A_x \cos \theta - A_z \sin \theta & K_y \xrightarrow{\theta A_z} K_y & K_y \xrightarrow{\left(\frac{\pi}{2}\right) K_y} K_y \\ 2A_zK_x \xrightarrow{\left(\frac{\pi}{2}\right) A_z} 2A_zK_x & 2A_zK_x \xrightarrow{\left(\frac{\pi}{2}\right) K_y} -2A_zK_z & 2A_xK_y \xrightarrow{\left(\frac{\pi}{2}\right) K_z} -2A_xK_x \\ 2A_yK_z \xrightarrow{\left(\frac{\pi}{2}\right) A_z} -2A_xK_z & 2A_yK_z \xrightarrow{\left(\frac{\pi}{2}\right) 2A_zK_z} -A_x & -K_x \xrightarrow{\phi 2A_zK_z} -K_x \cos \phi - 2A_zK_y \sin \phi \end{array}$$

Let's work through a complete example of the basic pulse-acquire experiment of Fig. 5 for a  $J$ -coupled system of two spins, which we analyzed classically in Fig. 12 to produce a doublet with the two lines separated by  $J$  Hz ( $2\pi J$  rad/s). Furthermore, let's assume  $A$  and  $K$  are different nuclides (e.g.  $A = {}^1\text{H}$  and  $K = {}^{13}\text{C}$ ) and the pulse is at the Larmor frequency of  $A$ , which means it has no effect on the  $K$  nuclei. Starting from thermal equilibrium and just focusing on the magnetization of the  $A$  nucleus, the pulse is applied:

The true thermal equilibrium state for the system is  $A_z + K_z$ , but it is common to simplify the analysis and focus only on terms of interest.

$$A_z \xrightarrow{\left(\frac{\pi}{2}\right)_{A_y}} A_x$$

Next the system precesses freely during the acquisition, which corresponds to evolution of the Hamiltonian, given in Eq. 13, for fixed periods of time,  $t$ . Since the Hamiltonian consists of terms expressed in units of rad/s, this means that each term rotates through a known angle during any given time interval. Therefore, in product operator notation the evolution of the free precession Hamiltonian corresponds to three rotations: the chemical shift of  $A$  ( $\Omega_A A_z$ ), the chemical shift of  $K$  ( $\Omega_K K_z$ ), and the  $J$ -coupling ( $\pi J t 2 A_z K_z$ ). However, the chemical shift of  $K$  has no effect on the system since there aren't any  $K$  terms that have  $x$ - or  $y$ -components. The other two effects can be worked in either order or together. First, look at them worked sequentially; below is the chemical shift:

$$A_x \xrightarrow{\theta_A A_z} A_x \cos \theta_A + A_y \sin \theta_A$$

where  $\theta_A = \Omega_A t$ . Next, the  $J$ -coupling is applied:

$$A_x \cos \theta_A + A_y \sin \theta_A \xrightarrow{\phi 2 A_z K_z} A_x \cos \theta_A \cos \phi + 2 A_y K_z \cos \theta_A \sin \phi + A_y \sin \theta_A \cos \phi - 2 A_x K_z \sin \theta_A \sin \phi \quad (22)$$

Relaxation effects have been neglected for simplicity. Eq. 30 technically states this system rotates in the  $xy$ -plane forever, but in practice it will eventually relax back to thermal equilibrium.

where  $\phi = \pi J t$ . Recall that the result is a complete description of the state of the system at any time,  $t$ , in terms of a set of basis operators. Even though this may look like a large number of terms, remember that the observed signal is simply the coefficient on the  $A_x$  term; at this point we can ignore all the other terms as they don't generate an observable signal on the detector. Using trigonometric identities the coefficient on the  $A_x$  term can be expressed in terms of individual frequency components:

$$\cos(\Omega_A t) \cos(\pi J t) = \frac{1}{2} [\cos((\Omega_A - \pi J) t) + \cos((\Omega_A + \pi J) t)]$$

So there are two frequency components in the FID: one with a frequency of  $\Omega_A + \pi J$  and the other with a frequency of  $\Omega_A - \pi J$ . This exactly matches the result described by Fig. 12, where the  $\alpha$  transition is displaced by  $+J/2$  Hz ( $+\pi J$  in angular units) and the  $\beta$  transition is displaced by  $-J/2$  Hz. Mathematically, the line shapes shown in Fig. 9 are the result of the Fourier transform applied to cos and sin functions. Positive absorptive corresponds to  $+\cos$ , negative absorptive corresponds to  $-\cos$ , and dispersive corresponds to  $\pm \sin$ . So the spectrum of the function above consists of an in-phase doublet where the two lines have a positive absorptive line shape and are separated by  $J$  Hz.

When you first learn the product operator formalism the analysis given above is beneficial to help solidify understanding of the individual steps. However, it can be cumbersome, particularly as the complexity of experiments increases, since there tends to be a lot of individual terms to keep track of. As you gain proficiency with the method you should look to start simplifying the process by working the chemical shift and  $J$ -coupling effects together, as shown below:

$$A_x \xrightarrow{\begin{matrix} \theta_A A_z \\ \phi 2 A_z K_z \end{matrix}} \left( \begin{matrix} A_x \cos \theta_A \\ + \\ A_y \sin \theta_A \end{matrix} \right) \cos \phi + \left( \begin{matrix} 2 A_y K_z \cos \theta_A \\ + \\ - 2 A_x K_z \sin \theta_A \end{matrix} \right) \sin \phi$$

The result is the same, obviously, but the form is much more compact, substantially easier to read, and easier to perform subsequent operations if the experiment were more complex.

### Difficulty with Nuclei Other Than $^1\text{H}$

$^1\text{H}$  NMR benefits from many advantages over most other NMR active nuclei: it has a high natural abundance and it has a large value for  $\gamma$ . The natural abundance of a nucleus directly relates to the observed signal.  $^1\text{H}$  nuclei are 99.98% abundant so the signal is essentially as large as it can be based on this parameter. When considering organic molecules the other most likely nuclei of interest are  $^{13}\text{C}$  (1.1% abundant,  $I = 1/2$ ),  $^{15}\text{N}$  (0.37% abundant,  $I = 1/2$ ), and  $^{17}\text{O}$  (0.037% abundant,  $I = 5/2$ ) which are substantially less abundant. Recall that the signal-to-noise ratio ( $S/N$ ) improves by  $N^{1/2}$ , so to get equivalent  $S/N$  between  $^1\text{H}$  and  $^{13}\text{C}$  the  $^{13}\text{C}$  spectrum would take  $100 \times 100 = 10,000$  times longer to acquire based only on the difference in abundance!

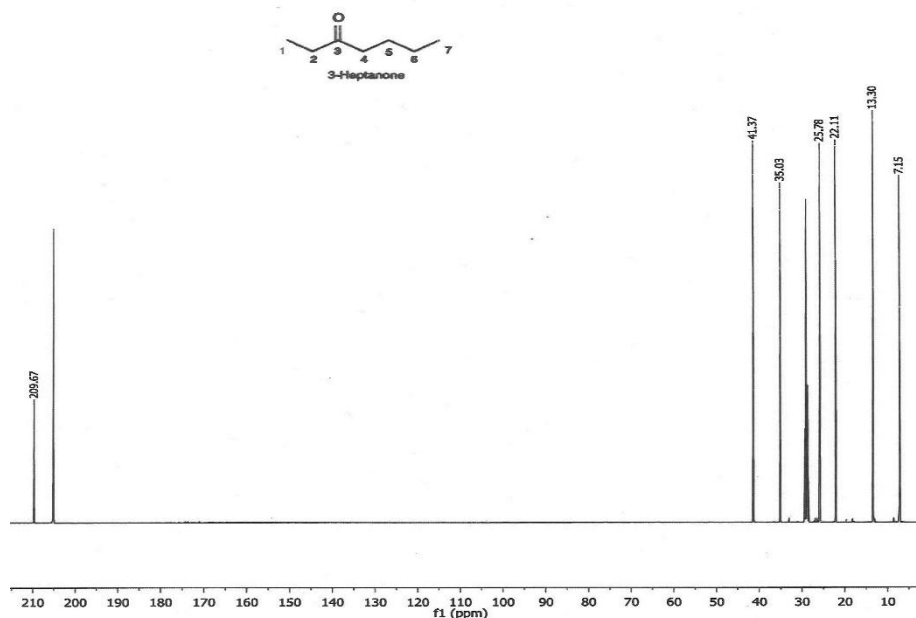
The observed  $S/N$  also depends on  $\gamma$ . In fact, it depends on  $\gamma^{5/2}$ . This total dependence on  $\gamma$  stems from four specific contributions:

- 1) *Boltzmann distribution*:  $\gamma$  affects the energy level spacing between the spin states (Eq. 5) which affects the population difference between the states and, thus, the magnitude of the net magnetization at thermal equilibrium. Net result:  $S \propto \gamma$ .
- 2) *Magnetic moment*:  $\gamma$  affects the size of the magnetic moment (Eq. 3) which affects the magnitude of the net magnetization. Net result:  $S \propto \gamma$ .
- 3) *Larmor frequency*:  $\gamma$  affects the Larmor frequency (Eq. 6) which affects the magnitude of the induced current in the detector element. Net result:  $S \propto \gamma$ .
- 4) *Noise*:  $\gamma$  affects the total bandwidth of the measurement (Eq. 7). Net result:  $N \propto \gamma^{1/2}$ .

These combine to give  $S/N \propto \gamma^{5/2}$ . Thus, considering  $^{13}\text{C}$ , which has a  $\gamma$  that is  $1/4$  that of  $^1\text{H}$ , the  $S/N$  for  $^{13}\text{C}$  is reduced by a factor of 32. Combined with the natural abundance issue discussed previously this means the overall  $S/N$  for  $^{13}\text{C}$  is 3200 times less than that for  $^1\text{H}$ , so to get spectra of equal  $S/N$  the  $^{13}\text{C}$  spectrum will take  $3200 \times 3200 \approx 10$  million times longer! Even if the  $^1\text{H}$  spectrum only took one second to acquire, the  $^{13}\text{C}$  spectrum would take about four months to complete (for same  $S/N$ )!

Because of this tremendous reduction in  $S/N$  it is common to employ one or more strategies to increase the signal. Spin-spin coupling provides valuable information about attached nuclei but that comes at the cost of splitting the signal into fragments. A 1:2:1 triplet, for example, has four times more intensity than the outer two peaks if the splitting is removed. So *decoupling* of the spectrum (by constant irradiation of the attached nuclei) is often performed. The constant irradiation mixes the state information of the connected nucleus and removes the splitting shown in Fig. 11 so  $\alpha$ -transitions are indistinguishable from  $\beta$ -transitions. Although the increase in  $S/N$  due to decoupling is substantial, and often needed to make observation of the signal even practical, remember that it comes at a great cost: information regarding connectivity, through the  $J$ -coupling interaction, is lost. Below are  $^{13}\text{C}$  spectra of 3-heptanone acquired with  $^1\text{H}$ -decoupling, designated as a  $^{13}\text{C}\{^1\text{H}\}$  spectrum, and without decoupling. The signals that are not labeled come from the solvent. Note that without the  $J$ -coupling information, very few assignments can be made.

You can think of decoupling as a constant series of  $\pi$ -pulses during the acquisition.



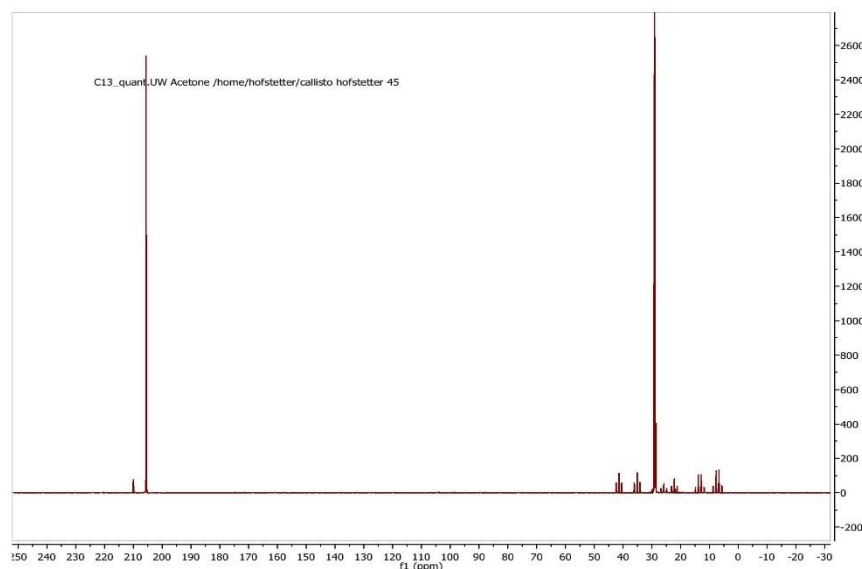


**Figure 17.**  $^{13}\text{C}\{^1\text{H}\}$  spectra of 3-heptanone: the standard decoupled acquisition (top) and a coupled acquisition (bottom). Signals without labels (28 ppm and 205 ppm) are from the solvent. Without  $J$ -coupling information, very few assignments can be made. Note the severe decrease in  $S/N$  in the coupled spectrum.

### Polarization Transfer

As just described, one of the difficulties acquiring data on nuclei other than  $^1\text{H}$  is due to the lower population difference between states due to the Boltzmann distribution at thermal equilibrium. However, this population difference can be manipulated through a process called *polarization transfer* where magnetization from one nucleus is transferred to a  $J$ -coupled neighbor. An example process is given below:

$$A_z \xrightarrow{\left(\frac{\pi}{2}\right)A_y} A_x \xrightarrow{\left(\frac{\pi}{2}\right)2A_zK_z} 2A_yK_z \xrightarrow{\left(\frac{\pi}{2}\right)A_x} 2A_zK_z \xrightarrow{\left(\frac{\pi}{2}\right)K_y} 2A_zK_x$$

Note that the starting  $A_z$  magnetization ends up as transverse  $K$  magnetization that can be detected and observed. The first, third and fourth steps can be accomplished with pulses that have the frequency and phase specified. The second step is accomplished through the  $J$ -coupling mechanism, which happens over time. As shown earlier, the general form of the  $J$ -coupling rotation is given as  $(\pi Jt)2A_zK_z$ . For an angle of  $\pi/2$  the time,  $t$ , must be  $1/(2J)$ . Putting it all together the corresponding full pulse sequence for the process above is written as:

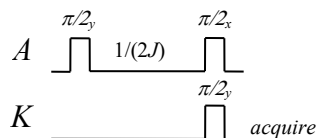


**Figure 18.** The fundamental pulse sequence to transfer polarization from nucleus  $A$  to nucleus  $K$ .

“Transverse” means  $x$ - or  $y$ -components. For example, operators like  $A_x$  and  $2A_yK_z$  represent transverse  $A$  magnetization, while operators like  $K_x$  and  $2A_zK_y$  represent transverse  $K$  magnetization.

It can be useful to use a shorthand line notation to track observable transverse magnetization. This is shown below:

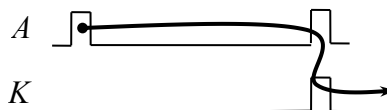


**Figure 19.** Shorthand line notation used to track observable transverse magnetization in a pulse sequence. In this example a transverse  $^1\text{H}$  component is generated and then transferred to its corresponding  $J$ -coupled  $^{13}\text{C}$  nucleus where it is observed.

The analysis of this pulse sequence given above neglected the evolution of the chemical shift,  $(\Omega_A t)A_z$ , during the  $1/(2J)$  delay. In practice, both the chemical shift and  $J$ -coupling evolve over any



passage of time. So what happens if the chemical shift of the  $A$  nucleus is included in the analysis? Below is the product operator description:

$$A_z \xrightarrow{\left(\frac{\pi}{2}\right)A_y} A_x \xrightarrow{\left(\frac{\pi}{2}\right)2A_zK_z} \begin{pmatrix} 2A_yK_z \cos\theta_A \\ -2A_xK_z \sin\theta_A \end{pmatrix} \xrightarrow{\left(\frac{\pi}{2}\right)(A_x+K_y)} \begin{pmatrix} 2A_zK_x \cos\theta_A \\ -2A_xK_x \sin\theta_A \end{pmatrix}$$

where  $\theta_A = \Omega_A t = \Omega_A/(2J)$ . As shown the amount of polarization transfer (given by the  $2A_zK_x$  term) is a function of the chemical shift, specifically a function of  $\cos\theta_A$ . The remaining magnetization becomes  $ZQ$  and  $DQ$  terms, given by the  $2A_xK_x$  term. As a physical interpretation, note that after the delay the  $A_\alpha$  and  $A_\beta$  vectors are antiphase but they can be anywhere in the  $xy$ -plane depending on the chemical shift ( $\Omega_A$ ). The subsequent  $A_x$  pulse only rotates the  $y$ -components to the  $z$ -axis, which is required for the polarization transfer;  $x$ -components are unaffected and lead to the creation of the  $ZQ/DQ$  components instead.

**Self Check #9:** Prove that all of the  $A$  magnetization transfers to the  $K$  nucleus for the case of  $\Delta_A = 0$ .

The product operator description given in the handout is

$$A_z \xrightarrow{\left(\frac{\pi}{2}\right)A_y} A_x \xrightarrow{\left(\frac{\pi}{2}\right)2A_zK_z} \begin{pmatrix} 2A_yK_z \cos\theta \\ -2A_xK_z \sin\theta \end{pmatrix} \xrightarrow{\left(\frac{\pi}{2}\right)A_x} \begin{pmatrix} 2A_zK_z \cos\theta \\ -2A_xK_z \sin\theta \end{pmatrix} \xrightarrow{\left(\frac{\pi}{2}\right)K_y} \begin{pmatrix} 2A_zK_x \cos\theta \\ -2A_xK_x \sin\theta \end{pmatrix}$$

where  $\theta = \Omega_A t = \Omega_A/(2J)$ .  $2A_zK_x$  is the polarization term, so whenever  $\cos\theta = \pm 1$ , all of the magnetization transfers to the  $K$  nucleus. When  $\Omega_A = 0$ ,  $\theta = 0$ , and  $\cos\theta = 1$ .

**Self Check #10:** Calculate a non-zero value for  $\Delta_A$  that results in complete polarization transfer.

Complete polarization transfer occurs when  $\cos\theta = \pm 1$ , which means  $\theta = n\pi$  where  $n$  is an integer.

$$\theta = \frac{\Omega_A}{2J} = \frac{2\pi\Delta_A}{2J} = n\pi$$

$$\therefore \Delta_A = nJ$$

So  $\Delta_A = J$  is a specific example of a non-zero value that results in complete polarization transfer.

**Self Check #11:** Calculate a non-zero value for  $\Delta_A$  that results in no polarization transfer. Is the resulting magnetization observable in the  $A$  frame?

The other term in the final state is the  $2A_xK_x$  term which is  $ZQ/DQ$  so it is unobservable in either frame. All of the magnetization is contained in this term when  $\sin\theta = \pm 1$ , which means  $\theta = (n + \frac{1}{2})\pi$  where  $n$  is an integer.

$$\theta = \frac{\Omega_A}{2J} = \frac{2\pi\Delta_A}{2J} = \left(n + \frac{1}{2}\right)\pi$$

$$\therefore \Delta_A = J\left(n + \frac{1}{2}\right)$$

So  $\Delta_A = J/2$  is a specific example of a non-zero value that results in no polarization transfer.

If the goal of the experiment is to perform a complete polarization transfer regardless of the chemical shift, how can this be accomplished? The chemical shift and  $J$ -coupling effects always operate on the state during any delay (free precession), and the chemical shift displaces the vectors in the  $xy$ -plane. The key is to reverse the chemical shift effect after half the delay. Then the chemical shift precesses back to its original location during the second half of the delay. This process is called a *spin echo*, and means an effect such as  $J$ -coupling or chemical shift “echoes” its original position at a given instant in time. The general concept of spin echoes is addressed in the next section, but let’s look at this specific application in more detail here. The modified pulse sequence, called INEPT, is shown below:

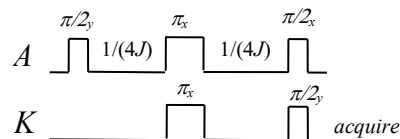


**Figure 20.** Expanded polarization transfer sequence that transfers a maximum amount regardless of offset frequency. This is the basic INEPT pulse sequence.

### Spin Echoes

Consider the pulse sequence snippet of  $-1/(4J) - \pi A_x, \pi K_x - 1/(4J) -$  starting from the  $A_x$  state and defining the angles  $\theta$  and  $\phi$  in terms of the total time, which is  $1/(2J)$ . The vector diagrams look like:

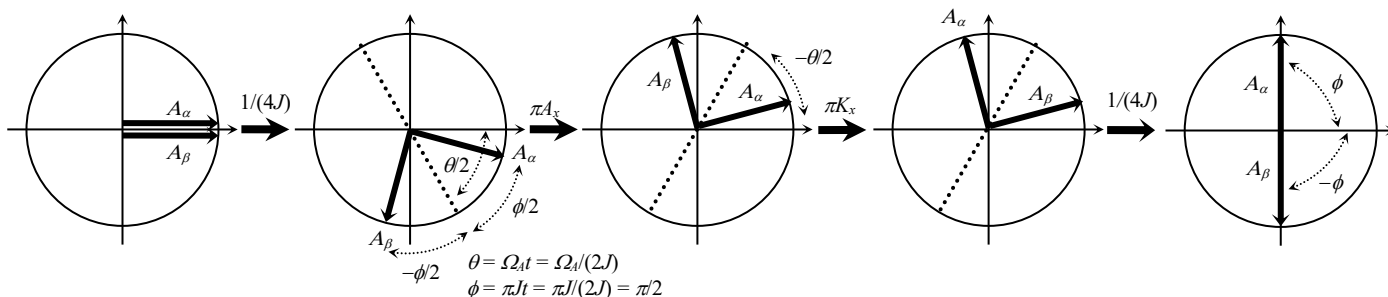


**Figure 21.** Vector diagrams of the magnetization for a  $J$ -coupled pair nuclei undergoing a sequence of  $-1/(4J) - \pi A_x, \pi K_x - 1/(4J) -$ . Note that the vectors end antiphase on the  $y$ -axis regardless of the chemical shift.

Note that the  $\pi A_x$  pulse rotates the  $A_\alpha$  and  $A_\beta$  vectors  $180^\circ$  around the  $x$ -axis and the  $\pi K_x$  pulse exchanges the vector labels. The effect of the  $\pi K_x$  on the  $A$  vectors may appear strange but can be understood either through a physical or a mathematical line of reasoning. From a physical perspective the  $\alpha$  and  $\beta$  labels on the vectors represent the spin state of the  $K$  nucleus and a  $\pi$  pulse on that nucleus completely converts those in the  $\alpha$  state to the  $\beta$  state, and vice versa; therefore  $A_\alpha$  exchanges with  $A_\beta$ . From a mathematical perspective the dephasing of the two vectors is represented by the  $2A_x K_z$  and the  $2A_y K_z$  operators and a  $\pi K_x$  pulse changes the sign of these terms, which is equivalent to exchanging the labels. The end result is that chemical shift echoes to its starting position but the  $J$ -coupling continues to evolve, resulting in a final rotation of  $\phi$ .

Writing the product operator description for the entire process is quite cumbersome and can distract from the overall process so a shortcut notation is used instead. Instead of following the individual pulses and delays, the entire spin echo is treated as a single rotation. For the example above this means it is treated as a single rotation of  $\phi 2A_z K_z$ . The  $\pi$  pulses must also be included, but the order doesn't matter. Thus, the product operator description for the example above is written as:

$$A_x \left( \frac{\pi(A_x + K_x)}{\rightarrow} A_x \frac{\left(\frac{\pi}{2}\right) 2A_z K_z}{\rightarrow} \right)^* 2A_y K_z$$

where the terms inside the  $()^*$  represent the spin echo. Note that although the  $\pi$  pulses do not affect the system in this case, it's possible that they introduce a negative sign in the process (consider a starting point of  $A_y$  instead of  $A_x$ ). So, it's still important to write them so the reader knows they have been considered.

Generalizing the spin echo as  $-\tau/2 - \pi A_x, \pi K_x - \tau/2 -$  where  $\tau$  is some arbitrary time period (e.g.  $\tau = 1/(2J)$  in the example above), it is evident that the sequence eliminates the effect of the chemical shift over the entire  $\tau$  period. This is an incredibly powerful tool since time delays in pulse sequences are generally in place to evolve either the chemical shift or the  $J$ -coupling, not both. For example, the  $1/(2J)$  delay in the INEPT sequence is used to evolve the  $J$ -coupling and convert the magnetization from in-phase to antiphase; evolution of the chemical shift is not desired. In total there are three different spin echoes for a heteronuclear (i.e.  $A$  and  $K$  are different nuclides) spin echo, and are shown below in Fig. 22:

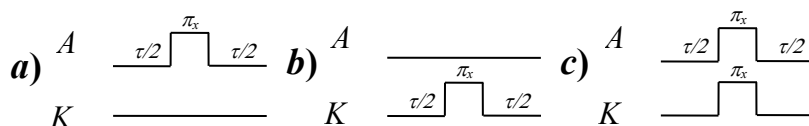
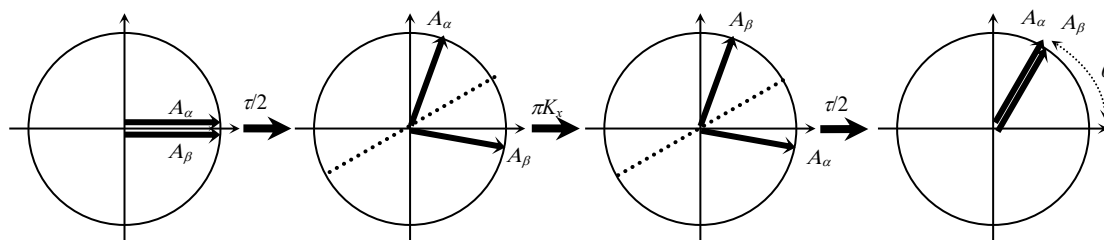


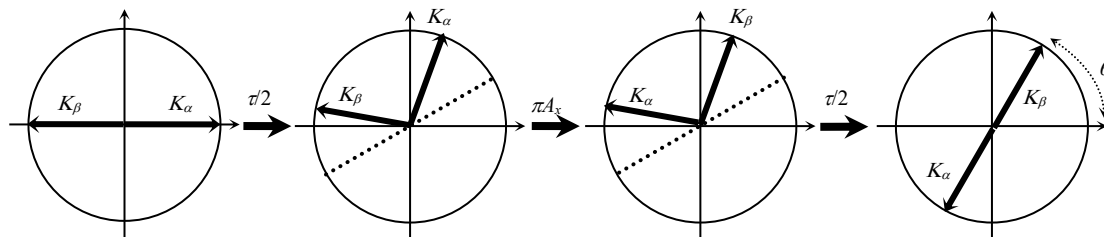
**Figure 22.** Three different schemes for generating a spin echo on a heteronuclear  $AK$  coupled pair.  
**a)** refocuses  $\theta_A$  and  $\phi$ , **b)** refocuses  $\theta_K$  and  $\phi$ , and **c)** refocuses  $\theta_A$  and  $\theta_K$

Depending on the sequence used, the effects of chemical shift and/or  $J$ -coupling can be effectively removed over any period of time. Below is an example set of vector diagrams, and corresponding product operator description, for Fig. 22b starting from the  $A_x$  operator with  $\theta = 60^\circ$  and  $\phi = 80^\circ$  for the  $\tau$  interval:



$$A_x \left( \xrightarrow{\pi K_x} A_x \xrightarrow{\theta A_z} \right)^* A_x \cos \theta + A_y \sin \theta$$

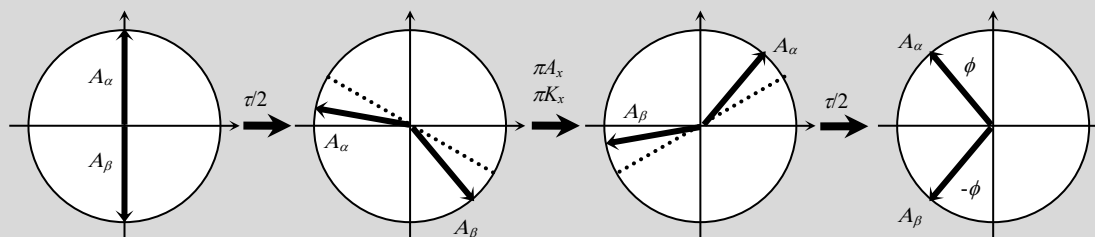
And as another example, below are the descriptions for Fig. 22a starting from the  $2A_zK_x$  operator with  $\theta = 60^\circ$  and  $\phi = 80^\circ$  for the  $\tau$  interval:



$$2A_zK_x \left( \xrightarrow{\pi A_x} -2A_zK_x \xrightarrow{\theta K_z} \right)^* -2A_zK_x \cos \theta + -2A_zK_y \sin \theta$$

In both examples above, the  $J$ -coupling is refocused and the chemical shift evolves over the entire delay for a final rotation angle of  $\theta$ .

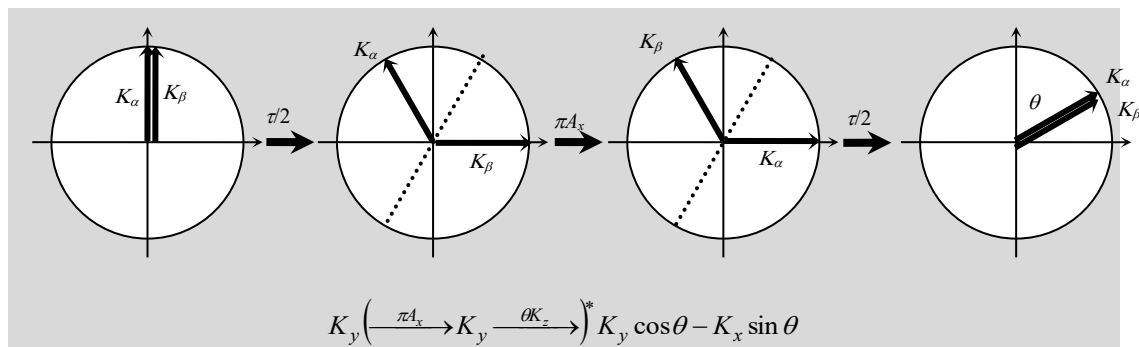
**Self Check #12:** Sketch a set of vector diagrams and give the product operator description for the pulse snippet given in Fig. 22c starting with the  $2A_yK_z$  operator. Use  $\theta = 120^\circ$  and  $\phi = 40^\circ$  for the  $\tau$  interval.



$$2A_yK_z \left( \xrightarrow{\pi(A_x+K_x)} 2A_yK_z \xrightarrow{\phi 2A_zK_z} \right)^* 2A_yK_z \cos \phi - A_x \sin \phi$$

As shown, the chemical shift ( $\theta$ ) refocuses but the  $J$ -coupling ( $\phi$ ) evolves throughout the entire sequence. The result is simply that the starting term,  $2A_yK_z$ , gets rotated by  $\phi 2A_zK_z$ .

**Self Check #13:** Sketch a set of vector diagrams and give the product operator description for the pulse snippet given in Fig. 22a starting with the  $K_y$  operator. Use  $\theta = -60^\circ$  and  $\phi = 120^\circ$  for the  $\tau$  interval.



As shown, the  $J$ -coupling ( $\phi$ ) refocuses but the chemical shift ( $\theta$ ) evolves throughout the entire sequence. The result is simply that the starting term,  $K_y$ , gets rotated by  $\theta K_z$ .

### RINEPT – Refocused Insensitive Nuclei Enhanced through Polarization Transfer

The basics of the INEPT sequence was presented earlier (Fig. 20), and is an example of using polarization transfer to enhance a signal from a less sensitive nuclide. Although the sequence works as given, it is not ideal. Recall that for insensitive nuclei such as  $^{13}\text{C}$  the spectrum is often acquired decoupled so that all of the signal intensity is in a singlet instead of spread out over a more complex multiplet, such as a quartet. Decoupling prevents evolution of the  $J$ -coupling and since the transferred magnetization at the end of the pulse sequence in Fig. 20 is antiphase, it won't evolve into an observable signal if the decoupler is used. Instead an extra delay must be added to refocus the antiphase components. Analogous to the first delay in the sequence, the goal of the delay is to allow the  $J$ -coupling to evolve without the effects of chemical shift, so another spin echo is required.

The full sequence is given below:

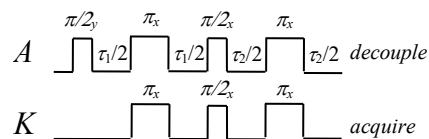


**Figure 23.** RINEPT sequence which allows decoupling to be used during acquisition.

where  $\tau_1 = 1/(2J)$  s. The value for  $\tau_2$  is addressed later but for now, assume  $\tau_1 = \tau_2 = 1/(2J)$  s. The product operator description of Fig. 23 is then:

$$A_z \xrightarrow{\left(\frac{\pi}{2}\right)A_y} A_x \left( \xrightarrow{\pi(A_x+K_x)} A_x \xrightarrow{\left(\frac{\pi}{2}\right)2A_zK_z} \right)^* 2A_yK_z \xrightarrow{\left(\frac{\pi}{2}\right)(A_x+K_x)} -2A_zK_y \left( \xrightarrow{\pi(A_x+K_x)} -2A_zK_y \xrightarrow{\left(\frac{\pi}{2}\right)2A_zK_z} \right)^* K_x$$

The concepts associated with each component in the pulse sequence of Fig. 23 can be visualized in a schematic form as shown below. In this format the text in each box provides the goal of that step, and in the case of acquisition it includes the information obtained. The text above each box describes any special conditions for that step which are accomplished using a spin echo. The text below describes the state or conversion of the desired magnetization as “I” for in-phase or “A” for antiphase.

Acquisition generally provides information about  $\Omega$  and  $J$  (as  $\Omega \pm \pi J$ ), but decoupling removes the  $J$ -coupling information.

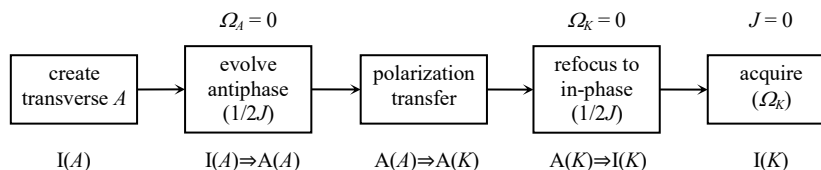


**Figure 24.** Conceptual schematic form of the RINEPT pulse sequence shown in Fig. 23.

Now let's consider the value for  $\tau_2$ . All  $-\text{CH}_n$  groups are doublets in the  $^1\text{H}$  spectrum (they couple to only one  $^{13}\text{C}$ ), but they have different multiplicities in the  $^{13}\text{C}$  spectrum. The individual components have different frequencies and therefore have different optimal rephasing times. This is shown in the table below:

Group	$^1\text{H}$ Signal	$^{13}\text{C}$ Signal	$^{13}\text{C}$ Frequency Components	RINEPT Signal Intensity ( $\phi = \pi J \tau_2$ )
$-\text{CH}$	doublet	doublet	$\pm J/2$	$\propto \sin(\phi)$
$-\text{CH}_2$	doublet	triplet	$\pm J$	$\propto \sin(2\phi)$
$-\text{CH}_3$	doublet	quartet	$\pm J/2, \pm 3J/2$	$\propto \sin(\phi) + \sin(3\phi)$

**Table 2.** Observed RINEPT signal intensity for the various  $-\text{CH}_n$  groups as a function of the refocusing time,  $\tau_2$ .

A plot of the signal intensity as a function of  $\phi$  is shown below:

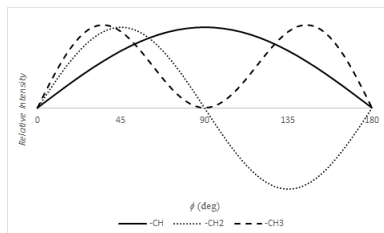


**Figure 25.** Relative RINEPT signal intensity as a function of the refocusing angle,  $\phi$ .

As shown, if  $\phi = 90^\circ$  ( $\tau_2 = 1/(2J)$ ) then the refocusing time is optimal for  $-\text{CH}$  groups but causes the other groups to be antiphase and therefore unobservable. From this plot there are three values for  $\tau_2$  that provide unique characteristics in the spectrum. These are summarized below:

$\phi$	$\tau_2$	Description
$45^\circ$	$1/(4J)$	All $-\text{CH}_n$ positive
$90^\circ$	$1/(2J)$	$-\text{CH}$ only
$135^\circ$	$3/(4J)$	$-\text{CH}$ , $-\text{CH}_3$ positive $-\text{CH}_2$ negative

**Table 3.** The three most common refocusing times used for RINEPT spectra.

An example RINEPT-135 spectrum (meaning  $\phi = 135^\circ$  and  $-\text{CH}_2$  groups are inverted) is shown below. This information, along with the fact that quaternary  $^{13}\text{C}$  are not present in the spectrum, allows for many more assignments to be made.

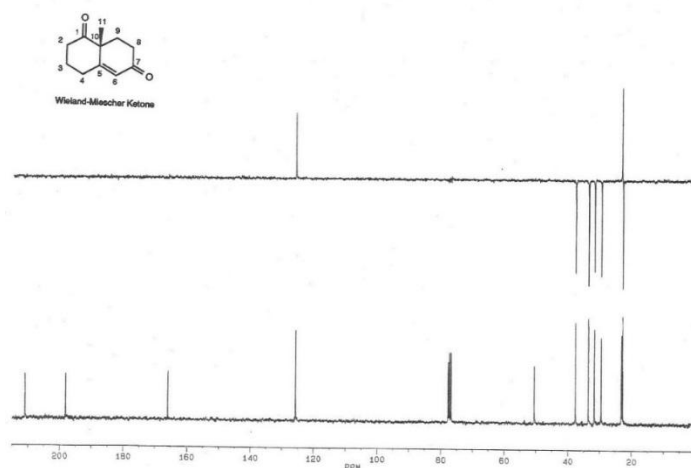
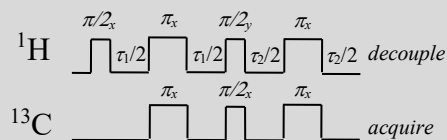


**Figure 26.** A combination of a RINEPT spectrum (top) and standard  $^{13}\text{C}\{^1\text{H}\}$  spectrum (bottom).  $^{13}\text{C}$  nuclei that do not have  $^1\text{H}$  attached are eliminated in the RINEPT and signals from  $-\text{CH}_2$  groups have negative intensity. The three signals at 77 ppm are from the solvent.

**Self Check #14:** The RINEPT sequence given in Fig. 23 converts  $A_z$  to  $K_x$ . If the first pulse is an  $x$ -pulse instead of a  $y$ -pulse, change the phase of the other pulses to accomplish the same goal.

There is not a unique solution, but a possible solution is shown below:



$$A_z \xrightarrow{\left(\frac{\pi}{2}\right)A_x} -A_y \left( \xrightarrow{\pi(A_x+K_x)} A_y \xrightarrow{\left(\frac{\pi}{2}\right)2A_zK_z} \right)^* -2A_xK_z \xrightarrow{\left(\frac{\pi}{2}\right)(A_y+K_x)} -2A_zK_y \left( \xrightarrow{\pi(A_x+K_x)} -2A_zK_y \xrightarrow{\left(\frac{\pi}{2}\right)2A_zK_z} \right)^* K_x$$

The change in the phase of the first pulse changes the antiphase operator at the point of the polarization transfer from  $2A_yK_z$  to  $-2A_xK_z$  which must get converted to  $-2A_zK_y$ . This is accomplished by changing the phase of the  $A$  pulse from  $x$  to  $y$ .

### Two-Dimensional Experiments

Acquiring an FID is a one-dimensional experiment: the induced current in the detection coil is measured as a function of time. As shown previously, the FID can contain a variety of information depending on the pulse sequence, but ultimately the information is limited due to the one-dimensional nature of the experiment. Consider a scenario where a series of FIDs are collected with a delay in the pulse sequence incremented between each one. Now each FID can be analyzed in the usual way, but also the progression of changes in the FIDs as a function of the altered delay can be examined, as shown in Fig. 27. This is the nature of a two-dimensional experiment and in practice the delay increments are made in a consistent manner so that a FT can be used to transform that time domain information into the frequency domain.

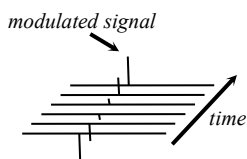


**Figure 27.** Concept of a two-dimensional experiment. Individual FIDs are acquired using a progression of values for a particular variable in the pulse sequence. After a FT of each FID, the signal amplitudes are modulated by the variable allowing for another FT point-by-point across the FIDs to put this information in the frequency domain.

By convention the acquisition of each FID is given the time domain designation  $t_2$  and is called the *direct dimension*. The variable delay in the pulse sequence is given the time domain designation  $t_1$  and is called the *indirect dimension*. For comparison, below is shown the simplest 1D (pulse-acquire experiment described earlier) and the simplest 2D experiment in the conceptual schematic form presented earlier:

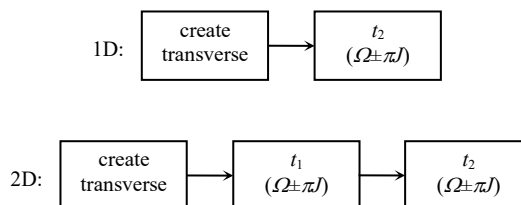
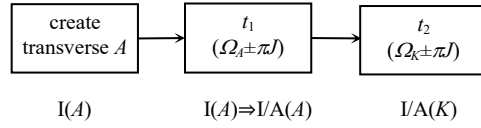


**Figure 28.** Conceptual schematic form of the simplest 1D (pulse-acquire) and the simplest 2D experiments. Note that during the  $t_2$  acquisition the magnetization can be in-phase or antiphase, unless decoupling is used in which case the magnetization would need to be in-phase at the start of the acquisition to be detected.

Although the 1D pulse-acquire experiment is commonly performed, the 2D sequence shown is only for illustrative purposes since it provides the same information in both dimensions (i.e. it doesn't provide any additional information relative to its 1D counterpart). Instead, other components are added to the 2D sequence so that the information content differs between the two dimensions. It is important to realize, though, that every 2D experiment must consist of at least the boxes shown in Fig. 28. The rest of the handout focuses on specific examples of some common 2D experiments.

The HETCOR experiment correlates signals that are spin-coupled together, where the two signals come from different nuclides (such as  $^1\text{H}$  and  $^{13}\text{C}$ ). Thinking about it conceptually, start with the template for a 2D experiment given in Fig. 28 and have the information for the nucleus be acquired during  $t_1$  and the information for the  $K$  nucleus acquired during  $t_2$ . This leads to a starting pulse on the  $A$  nucleus to create the transverse magnetization, as shown below:



You should see that there is a problem in that the  $t_1$  and  $t_2$  sections do not match up; the magnetization is on the  $A$  nucleus during  $t_1$  and we need it on the  $K$  nucleus during  $t_2$ . This can be accomplished by adding a polarization transfer step:

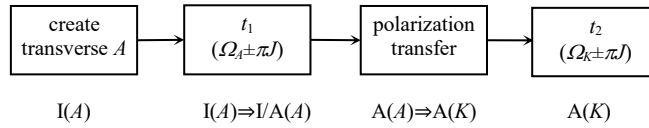


**Figure 29.** Conceptual schematic form of the HETCOR experiment.

Transforming the concepts above into a pulse sequence yields the general sequence given below, shown in the shortcut line notation used previously:

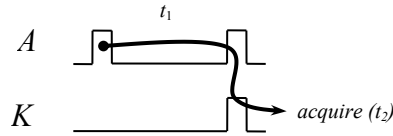


**Figure 30.** Line notation for the HETCOR pulse sequence. The magnetization is on the  $A$  nucleus during  $t_1$  and on the  $K$  nucleus during  $t_2$ .

Phases for the pulses would have to be chosen to route the magnetization properly through the sequence and end with the desired term for detection. There is not a unique choice, but one such choice is given in the final sequence below:

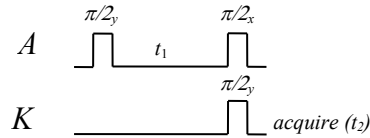


**Figure 31.** The simplest heteronuclear shift correlation experiment.

The product operator description looks like:

$$\begin{aligned}
 A_z &\xrightarrow{\left(\frac{\pi}{2}\right)A_y} A_x \xrightarrow{\frac{\theta_{A1}A_z}{\phi_1 2A_zK_z}} \left( A_x \cos \theta_{A1} \right) \cos \phi_1 + \left( 2A_yK_z \cos \theta_{A1} \right) \sin \phi_1 \\
 &\xrightarrow{\left(\frac{\pi}{2}\right)(A_x+K_y)} \left( A_x \cos \theta_{A1} \right) \cos \phi_1 + \left( 2A_zK_x \cos \theta_{A1} \right) \sin \phi_1
 \end{aligned}$$

where  $\theta_{A1} = \Omega_{A1}t_1$  and  $\phi_1 = \pi J t_1$ . The only observable term is  $2A_zK_x \cos \theta_{A1} \sin \phi_1$  which explicitly gives the frequency dependence of  $f_1$  to be  $\Omega_{A1} \pm \pi J$  (from the trig. identity for the cos/sin multiplication). The frequency dependence of  $f_2$  can be inferred from the product operator: the  $2A_zK_x$  operator will get tagged with cos or sin components of  $\theta_{K2} = \Omega_{K2}t_2$  and  $\phi_2 = \pi J t_2$  during  $t_2$  and result in frequencies of  $\Omega_{K2} \pm \pi J$ . Note that if line shape is of interest then you would need to

know the specific cos/sin terms, but generally for 2D experiments only the frequencies of the signals are of interest.

This simple version of the pulse sequence is ultimately not ideal because the spectrum consists of multiplets in both dimensions ( $J$ -coupling evolves during both  $t_1$  and  $t_2$ ), meaning the total signal intensity is spread out over many individual components. Ideally this coupling is removed in both dimensions so the signal is just a singlet that has a frequency of  $\Omega_A$  in  $f_1$ , and a frequency of  $\Omega_K$  in  $f_2$ . The specifics of the modifications are left as an activity later in the experiment. A HETCOR of 3-heptanone is shown below. Note that when combined with the  $^1\text{H}$  assignments made from the COSY the entire  $^{13}\text{C}$  spectrum can be assigned.

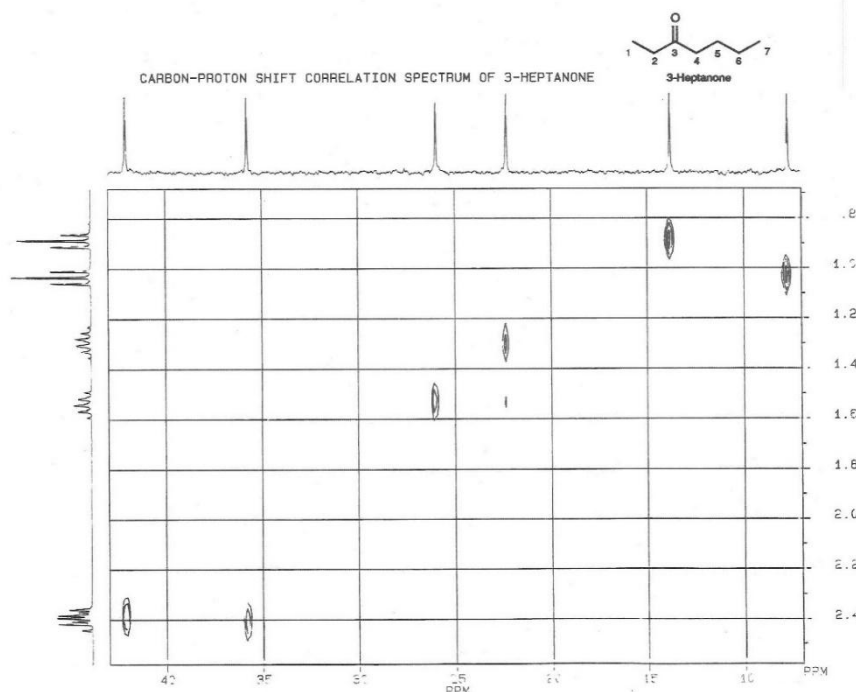


**Figure 32.** HETCOR spectrum of 3-heptanone. Combined with complete assignment of the  $^1\text{H}$  spectrum through the use of the COSY spectrum, all of the  $^{13}\text{C}$  assignments can be made.

#### *COSY – Correlated Spectroscopy (i.e. Homonuclear Shift Correlation)*

Although the previous discussion focused on transferring polarization from  $^1\text{H}$  to  $^{13}\text{C}$ , the process of polarization transfer occurs for any spin-coupled through the antiphase operators. So polarization transfer can occur between nuclei of the same type (called a *homonuclear* situation). So the COSY sequence is actually the same as the simple HETCOR sequence shown above, except it's important to note that each pulse affects both  $A$  and  $K$ ; they cannot be pulsed separately.

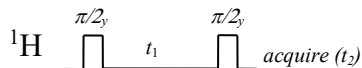


**Figure 33.** COSY pulse sequence for  $^1\text{H}$  two-dimensional homonuclear shift correlation.

For as simple as the pulse sequence looks, the information content is substantially more complex as evidenced by examining the corresponding line notation:

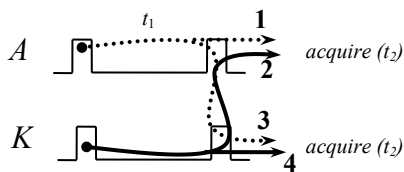


**Figure 34.** Shorthand line notation for the COSY pulse sequence. There are 4 unique pathways that lead to observable signals in the spectrum. The solid lines track the starting  $K_x$  magnetization and the dotted lines track the starting  $A_z$  magnetization. The second pulse causes some of the antiphase magnetization of each nucleus to transfer to the other one.



The first set of pulses creates transverse magnetization for both nuclei that evolve with their corresponding chemical shift during  $t_1$ . Depending on the specific value of  $t_1$  for each FID, there will be in-phase and anti-phase components immediately before the second set of pulses. After the second set of pulses the in-phase components continue to evolve during  $t_2$  with the same chemical shift they had during  $t_1$ . These components are illustrated by the top and bottom arrows at the end of the sequence. The anti-phase components, however, transfer to the other nucleus and evolve during  $t_2$  with the chemical shift of the opposite nucleus than it had during  $t_1$ . These components are illustrated by the middle arrows at the end of the sequence. As shown, there are a total of 4 pathways that provide observable signals, each with unique information content. These are summarized in the table below:

	Information Content	
Pathway	$t_1$	$t_2$
<b>1</b>	$\Omega_A \pm \pi J$	$\Omega_A \pm \pi J$
<b>2</b>	$\Omega_K \pm \pi J$	$\Omega_A \pm \pi J$
<b>3</b>	$\Omega_A \pm \pi J$	$\Omega_K \pm \pi J$
<b>4</b>	$\Omega_K \pm \pi J$	$\Omega_K \pm \pi J$

**Table 4.** Information content of the 4 unique pathways present in the COSY experiment.

Pathways **1** and **4** result in signals with the same frequency in each dimension and are therefore called *diagonal peaks* as they reside on a line where  $f_1 = f_2$ . Pathways **2** and **3** result in signals that have undergone polarization transfer between  $t_1$  and  $t_2$ , and therefore have different frequency information in the two dimensions. These are called *off-diagonal peaks* and illustrate  $J$ -coupled signals.

Even though this analysis is specifically for a system of only two homonuclear spin-coupled nuclei it can be extended to large molecules: every spin-coupled pair of nuclei in the molecule will produce a set of four peaks, two diagonal and two off-diagonal. Below is a COSY spectrum of 3-heptanone. Compare it to the simple  $^1\text{H}$  spectrum presented earlier. Note that with the COSY spectrum the signals for the two methyl groups can be assigned, which was not possible with the one-dimensional spectrum.

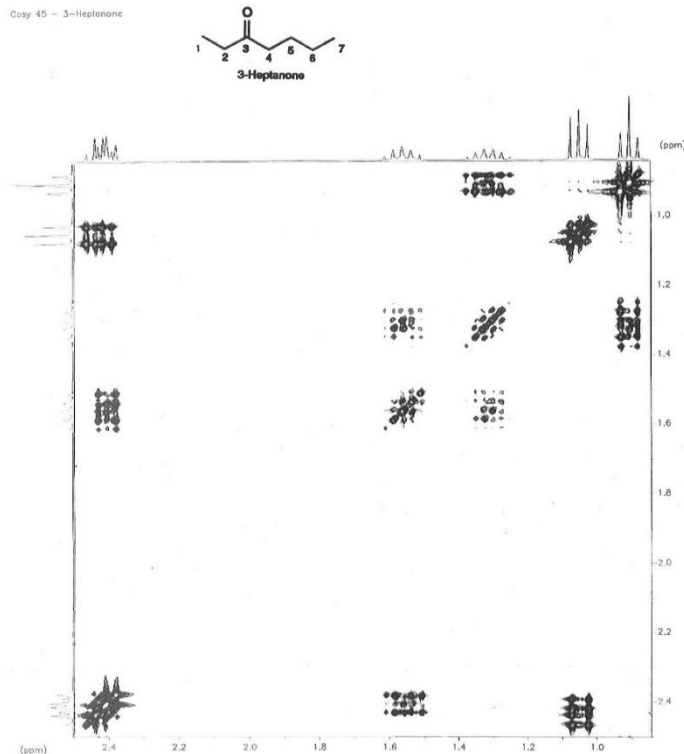


**Figure 36.** COSY spectrum of 3-heptanone. Peaks on the diagonal represent the basic  $^1\text{H}$  spectrum. Off-diagonal peaks connect diagonal peaks that are spin-coupled to each other. With this information the two methyl peaks can be assigned conclusively.

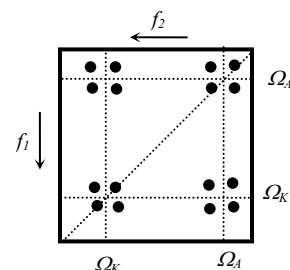


**Figure 35.** Results from a COSY experiment. The 2D FT consists of a set of diagonal and off-diagonal peaks. The diagonal peaks represent the normal  $^1\text{H}$  spectrum. The off-diagonal peaks connect signals that are spin-coupled with each other.

### Useful Trigonometric Identities

The following trigonometric identities are commonly used in NMR spectroscopy, particularly when using product operator descriptions:

$$\cos u = \cos(-u)$$

$$\sin u = -\sin(-u)$$

$$\cos^2 u + \sin^2 u = 1$$

$$\cos(2u) = \cos^2 u - \sin^2 u$$

$$\sin(2u) = 2 \sin u \cos u$$

$$\cos u \cos v = \frac{1}{2} [\cos(u - v) + \cos(u + v)]$$

$$\sin u \sin v = \frac{1}{2} [\cos(u - v) - \cos(u + v)]$$

$$\sin u \cos v = \frac{1}{2} [\sin(u + v) + \sin(u - v)]$$

$$\cos u \sin v = \frac{1}{2} [\sin(u + v) - \sin(u - v)]$$

### Using the NMR Visualization Software

- ☐ The first line specifies the starting state for the simulation. The overall syntax is: “START <#A<sub>z</sub>> <#K<sub>z</sub>>”. So to specify a starting state of A<sub>z</sub> + K<sub>z</sub>, you would use “START 1 1”. There are cases where you might want to start with just A<sub>z</sub>, in which case you would use “START 1 0”.
- ☐ The next lines specify the steps in the pulse sequence, which are either delays or pulses specified by the first character being either a D or P, respectively.
- ☐ For a delay, the next value is the length of the delay in ms. The overall syntax is: “D <delay>”. Example: “D 2.5” specifies a 2.5 ms delay.
- ☐ For a pulse, the next value is the angle of the pulse in degrees. This is then followed by two characters specifying the phase of the pulse for the A channel and the K channel, respectively. Phases are X, Y, -X, -Y, or N if the no pulse should be applied to that channel. The overall syntax is: “P <angle> <A phase> <K phase>”. Example: “P 90 Y N” specifies a 90° y-pulse on the A nucleus.
- ☐ After specification of the pulse-delay train, the acquisition is specified by “ACQ A” or “ACQ K” for acquiring A or K data, respectively.
- ☐ The decoupler can be specified similarly, using “DEC”. Note that the decoupling must be specified after the acquisition channel and automatically decouples the opposite channel from acquisition.
- ☐ The data may be visualized during the pulse sequence or the data acquisition by selecting the appropriate radio button and using the *Forward* and *Back* buttons.
- ☐ Trajectories for the next+previous steps can be shown by the check box.
- ☐ Any change to the spin system or pulse sequence requires hitting the *Calculate* button to recalculate the new states.

## Day 1 Activities

- 1.1. *Classical picture of a single spin:* Fig. 2 illustrates the “double-cone” classical picture of  $I = \frac{1}{2}$  nuclei in an external magnetic field. Calculate the tilt angle (angle between the magnetic moment and the  $z$ -axis) for each state. Now consider nuclei with  $I = 1$  (e.g.  $^{14}\text{N}$ ), and  $I = 5/2$  (e.g.  $^{17}\text{O}$ ). For each of these cases: 1) sketch diagrams similar to Fig. 1 and Fig. 2; and 2) calculate the tilt angles for each state.

*All remaining activities pertain to a coupled system of two nuclei ( $AK$ ), each of which has  $I = \frac{1}{2}$ .*

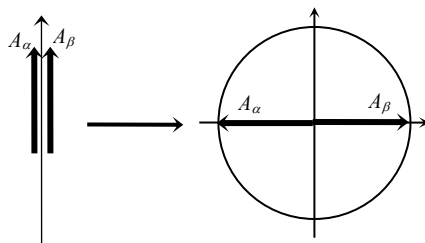
- 1.2 *Energy levels and transitions:* Sketch the energy levels of the system for the following three cases: 1)  $\gamma_A > \gamma_K$ , 2)  $\gamma_A < \gamma_K$ , and 3)  $\gamma_A = \gamma_K$ . Identify and label the transitions that can be driven using a pulse of EM radiation. Make sure to label the states and the transitions. What does the  $\alpha$  refer to in the  $K_\alpha$  transition? In one of the sketches, indicate with an arrow how  $J$ -coupling affects each energy level (assume  $J > 0$ ).
- 1.3 *Pulse-acquire:* Use the visualization software to explore the basic pulse-acquire experiment. You may want to review the brief instructions for the software given at the bottom of page 26. Start with the default parameters and verify that you understand: 1) how the magnetization evolves due to the pulse, 2) how the magnetization evolves during acquisition, 3) how the FID is determined from the magnetization, and 4) how the lineshape in the spectrum is determined from the position of the magnetization at the start of acquisition (see Fig. 9). Try changing a variety of parameters. Here are some suggestions: 1) change the offset frequency ( $\Delta_A$ ), 2) change the value of  $J$ , and 3) change the axis of the pulse.
- 1.4 *Pulse-delay-acquire:* For this exercise you will add a delay after the initial pulse but before the acquisition, just like the scenario in *Self-Check #4*. For the following scenarios: sketch classical vector diagrams for each step in the sequence, predict the spectrum, and then use the visualization software to verify your predictions:

Scenario #1:  $\Delta_A = 0, J = 100$  Hz: delays of 5 ms and 10 ms.

Scenario #2:  $\Delta_A = 50$  Hz,  $J = 100$  Hz: delays of 2.5 ms and 5 ms.

You should notice that in the cases where the delay is 5 ms, the two vectors evolve from the starting situation of being in-phase to being completely antiphase ( $180^\circ$ , or  $\pi$  radians, apart). What angle of  $\phi$  (see Fig. 12) does this evolution correspond to? For an arbitrary value of  $J$ , how much time does it take to evolve this angle (recall  $\phi = \pi Jt$ )?

- 1.5. *Pulse sequencing:* Design a pulse sequence (series of pulses and/or delays) to make the following conversion:



Use  $\Delta_A = \Delta_K = 0$  and  $J = 50$  Hz. Your sequence should contain the fewest number of pulses and delays, and their values should be the smallest possible.

- 1.6. *Failure of classical model:* From your solution to 1.5, add a  $\pi/2$   $y$ -pulse on the  $A$  nucleus after the delay. Make a classical prediction of the state of the system after the added pulse. Use the software to visualize the true state of the system and note the differences from the classical prediction.

You will learn a quantum mechanical approach in the next session which will correctly predict the experimental result for a scenario such as this one.

*Present activity 1.4 or 1.5 to a staff member, followed by a brief discussion.*

## Day 2 Activities

- 2.1.  $I_z$  operator: Recall that the wave functions can be specified by their quantum numbers as  $|l, m\rangle$  and that they are eigenfunctions of the  $I_z$  operator:  $I_z|l, m\rangle = m|l, m\rangle$ . Also recall that  $|\alpha\rangle$  and  $|\beta\rangle$  are used as abbreviations for  $|\frac{1}{2}, \frac{1}{2}\rangle$  and  $|\frac{1}{2}, -\frac{1}{2}\rangle$ , respectively. Complete the following relationships:

$$\begin{array}{ll} I_z|1, 1\rangle = ?? & I_z|\frac{5}{2}, -\frac{3}{2}\rangle = ?? \\ I_z|\alpha\rangle = ?? & I_z|\beta\rangle = ?? \end{array}$$

- 2.2.  $I_+$  and  $I_-$  operators: The raising and lowering operators ( $I_+$  and  $I_-$ , respectively) change the value of  $m$  in the wave function:  $I_+|l, m\rangle = |l, m+1\rangle$  and  $I_-|l, m\rangle = |l, m-1\rangle$ . A couple of specific examples are:  $I_+|1, 0\rangle = |1, 1\rangle$  and  $I_-|1, 0\rangle = |1, -1\rangle$ . Note that  $m$  has bounds, so if the operation were to take  $m$  out of bounds then the result vanishes. As examples,  $I_+|1, 1\rangle = 0$  and  $I_-|1, -1\rangle = 0$ . Complete the following relationships:

$$\begin{array}{ll} I_+|\alpha\rangle = ?? & I_+|\beta\rangle = ?? \\ I_-|\alpha\rangle = ?? & I_-|\beta\rangle = ?? \end{array}$$

- 2.3.  $I_x$  and  $I_y$  operators: As mentioned in the handout, the basis set wave functions that are eigenfunctions of  $I_z$  are not eigenfunctions of  $I_x$  and  $I_y$ .  $I_x$  and  $I_y$  can be defined in terms of the raising and lowering operators presented in the previous activity:  $I_x = (I_+ + I_-)/2$  and  $I_y = i(I_- - I_+)/2$ . Complete the following relationships:

$$\begin{array}{ll} I_x|\alpha\rangle = ?? & I_y|\alpha\rangle = ?? \\ I_x|\beta\rangle = ?? & I_y|\beta\rangle = ?? \end{array}$$

Lastly, use the relationships above to derive the matrix form of  $I_x$  and  $I_y$ . You may want to review the process shown for the derivation of the  $I_z$  matrix given at the top of page 9.

- 2.4. *Product operators #1*: Write the matrices for the following operators:  $A_z$ ,  $K_z$ , and  $2A_zK_z$ . Calculate and sketch the corresponding classical vector models for these operators. For each operator, sketch an energy level diagram, write in the populations given by the diagonal elements of the matrix and demonstrate consistency with the  $z$ -component of the vector diagram.
- 2.5. *Product operators #2*: Write the matrices for  $A_y$  and  $2A_xK_z$ . Calculate and sketch the corresponding classical vector models for these operators.
- 2.6. *Product operators #3*: Based on the examples in 2.4 and 2.5, sketch classical vector models for  $K_x$  and  $2A_zK_y$  without calculating the matrix form.
- 2.7. *Interpreting the density matrix*: Sketch the corresponding classical vector model for the following arbitrary density matrix. Keep track of the relative magnitudes of the vectors.

$$\frac{1}{2} \begin{pmatrix} 4 & -i & 0 & 0 \\ i & 4 & 0 & 0 \\ 0 & 0 & -4 & 1 \\ 0 & 0 & 1 & -4 \end{pmatrix}$$

- 2.8. *Basic rotations*: Fill in the missing information for each of the following basic rotations. You may find the rotation relationships on pages 12-13 helpful.

$$\begin{array}{ll} A_x \xrightarrow{\theta A_z} ?? & A_x \xrightarrow{??} A_x \cos \phi + 2A_yK_z \sin \phi \\ K_x \xrightarrow{??} K_z & ?? \xrightarrow{(\pi/2)2A_zK_z} K_y \\ 2A_zK_y \xrightarrow{??} 2A_zK_z & 2A_zK_z \xrightarrow{(\pi/2)A_y} ?? \end{array}$$

2.9. *Pulse sequencing*: Below is an example sequence of rotations that converts  $A_z$  to  $K_x$  when  $\Delta_A = \Delta_K = 0$ . For each step, fill in the missing rotation information and specify whether the rotation is accomplished experimentally with a pulse or a delay. Sketch the full pulse sequence. Enter the sequence into the visualization software and verify functionality.

$$A_z \xrightarrow{??} -A_y \xrightarrow{??} 2A_x K_z \xrightarrow{??} 2A_z K_z \xrightarrow{??} -2A_z K_y \xrightarrow{??} K_x$$

2.10. *Spectra*: Assign as many peaks as possible in spectra #1, 2, and 5. Explain your reasoning.

*Present activity 2.4, 2.5, or 2.9 to a staff member, followed by a brief discussion.*

### Day 3 Activities

3.1. *Acquisition #1*: Consider a pulse sequence that puts the system into a state described by  $K_x$  at the start of data acquisition.

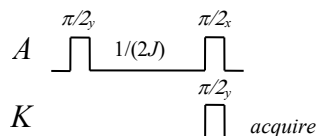
- Sketch the classical vector representation of the state.
- Predict the spectrum based on the classical model of NMR (use Fig. 9).
- Write a mathematical expression that corresponds to your prediction in part b. Note that the information presented on page 14 correlates the various line shapes in Fig. 9 to mathematical functions.
- Write the product operator notation for the acquisition. Note that this will be similar to the example worked through on page 14. Compare this derived mathematical expression to the predicted expression written in part c.
- Repeat parts b-d for a scenario where decoupling is used during the acquisition.

3.2. *Acquisition #2*: Consider a pulse sequence that puts the system into a state described by  $2A_x K_z$  at the start of data acquisition.

- Sketch the classical vector representation of the state.
- Predict the spectrum based on the classical model of NMR (use Fig. 9).
- Write a mathematical expression that corresponds to your prediction in part b.
- Write the product operator notation for the acquisition. Compare this derived mathematical expression to the predicted expression written in part c.
- Repeat parts b-d for a scenario where decoupling is used during the acquisition.

3.3. *Observables*: A product operator is said to be observable if it leads to the observation of spectral lines during the acquisition. Specify the product operators that are observable in an  $A$  spectrum and those that are observable in a  $K$  spectrum. How do the observables change if decoupling is used?

3.4. *Polarization Transfer*: Consider the pulse sequence from Fig. 18, shown below:



- Write the product operator notation for the sequence starting from  $4A_z + K_z$ , which is the quantitative representation of thermal equilibrium for a  $^1\text{H}$ - $^{13}\text{C}$  coupled pair.
- Identify the observable terms in the final state (i.e. the terms that generate a response on the detector).
- Predict the spectrum observed for the following three conditions: 1)  $\Delta_A = 0$ , 2)  $\Delta_A = J/2$ , and 3)  $\Delta_A = J$ . Use the classical model for your predictions. You will run this pulse sequence in the laboratory during the next period.

3.5. *Spectra*: Assign as many peaks as possible in spectra #7 and 10. Explain your reasoning.

*Present activity 3.1, 3.2, or 3.4 to a staff member, followed by a brief discussion.*

#### Day 4 Activities

- 4.1. *Spin echo #1*: Sketch a set of vector diagrams for Fig. 22b starting from  $A_y$ . Use  $\theta = -60^\circ$  and  $\phi = 160^\circ$  for the  $\tau$  interval. Write the product operator description for the sequence using the shorthand notation shown for the RINEPT sequence (Fig. 23) earlier in the handout. Keep  $\theta$  and/or  $\phi$  arbitrary in the description.
- 4.2. *Spin echo #2*: Sketch a set of vector diagrams for Fig. 22c starting from  $2A_yK_z$ . Use  $\theta = 120^\circ$  and  $\phi = 40^\circ$  for the  $\tau$  interval. Write the shorthand product operator description for the sequence.
- 4.3. *Spin echo #3*: Sketch a set of vector diagrams for Fig. 22a starting from  $2A_zK_x$ . Use  $\theta = 60^\circ$  and  $\phi = 20^\circ$  for the  $\tau$  interval. Write the shorthand product operator description for the sequence.
- 4.4. *Pulse sequencing #1*: Design a spin echo to evolve the chemical shift and eliminate the effects of  $J$ -coupling during an arbitrary time delay,  $t_1$ , for transverse  $K$  magnetization. Sketch a set of vector diagrams and write the shorthand product operator description for the echo, starting from  $K_x$ .
- 4.5. *Pulse sequencing #2*: Design a pulse sequence to convert  $K_z$  to  $2A_zK_y$  for any arbitrary value of the chemical shift and  $J = 50$  Hz. Sketch a set of vector diagrams and write the product operator description, using shorthand notation for any echoes.
- 4.6. *RINEPT*: Sketch a set of classical vector diagrams for the RINEPT pulse sequence given in Fig. 23 starting from  $A_z$  for the following conditions:  $\tau_1 = \tau_2 = 5$  ms,  $J = 100$  Hz,  $\Delta_A = 33.33$  Hz, and  $\Delta_K = -66.67$  Hz. Use the software to verify your sketches are correct at every point in the sequence. Explain why the value for  $\Delta_A$  does not affect the amount of polarization transfer.
- 4.7. *Spectra*: Assign as many peaks as possible in spectrum #12. Explain your reasoning.

*Present activity 4.4 or 4.5 to a staff member, followed by a brief discussion.*

#### Day 5 Activities

- 5.1. *HETCOR #1*: Write the product operator description for the HETCOR sequence of Fig. 31 starting from  $A_z$ . Identify the frequency terms in the  $f_1$  and  $f_2$  dimensions for each observable term. Sketch the spectrum.
- 5.2. *HETCOR #2*: As described in the handout, the HETCOR sequence of Fig. 31 is not ideal since the total signal is divided into four components but the information is such that it could be presented as a singlet ( $f_1 = \Omega_A$ , and  $f_2 = \Omega_K$ ). Design a pulse sequence to produce this frequency response. Note that the  $J$ -coupling dependence in  $f_1$  can be removed with the appropriate spin echo and the  $J$ -coupling dependence in  $f_2$  can be removed using the decoupler. The goal of the sequence can be viewed as converting  $A_z$  to  $K_x \cos(\Omega_A t_1)$ . Write the product operator description of your sequence.
- 5.3. *HSQC*: The sensitivity of the HETCOR experiment can be improved further by detecting the final magnetization as  $A$  instead of  $K$ , which is the HSQC experiment. To design this pulse sequence, convert  $A_z$  to  $A_x \cos(\Omega_K t_1)$  and use decoupling of the  $K$  nucleus during acquisition. Write the product operator notation, identify the  $f_1$  and  $f_2$  frequency components, and sketch the spectrum. The S/N for HETCOR is written as  $\gamma_A \cdot \gamma_K^{3/2}$  whereas the S/N for HSQC is written as  $\gamma_A \cdot \gamma_A^{3/2}$ . Therefore, for the case where  $A$  is  $^1\text{H}$  and  $K$  is  $^{13}\text{C}$  the HSQC experiment is 8 times more sensitive, which means it is 64 times faster. Ask a staff member for further clarification if these S/N terms are confusing.
- 5.4. *Spectra*: Assign as many peaks as possible in spectra #3 and 4. Explain your reasoning.

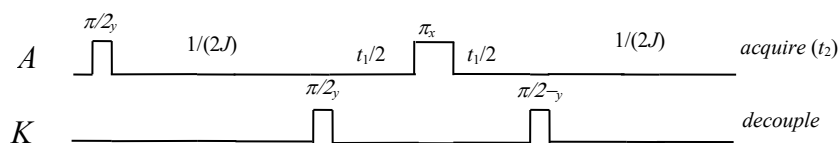
*Present activity 5.1, 5.2, or 5.3 to a staff member, followed by a brief discussion.*

## Day 6 Activities

### 6.1. COSY:

- Write the product operator description for the COSY sequence given in Fig. 33 starting from  $A_z + K_z$ . Note that the system is a coupled pair of  $^1\text{H}$  nuclei instead of a  $^1\text{H}$ - $^{13}\text{C}$  pair.
- Clearly identify the frequency terms in the  $f_1$  and  $f_2$  dimensions for each observable term.
- Sketch the spectrum.

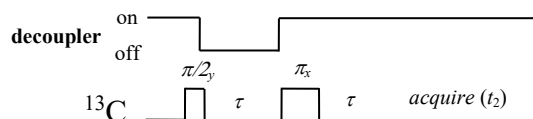
6.2. *HMQC*: Another popular experiment similar to HSQC is called HMQC. It produces the same results as HSQC but does not use any polarization transfer steps; instead it utilizes the multiple quantum operators (those with  $x$ - and  $y$ - components for both  $A$  and  $K$ ). Below is the typical pulse sequence:



Both sequences take the same amount of time, but HMQC has fewer pulses since spin echoes are not required during the  $1/(2J)$  delays.

- Write the product operator notation for the sequence, starting from  $A_z$ . To do this it is important to note that multiple quantum operators (such as  $2A_xK_x$ ) are not affected by  $J$ -coupling but are affected by both chemical shift rotations.
- Explain why spin echoes during the  $1/(2J)$  delays are required in HSQC but not in HMQC.

6.3. *APT*: In the handout you learned the RINEPT sequence which enhances a  $^{13}\text{C}$  spectrum through polarization transfer from attached  $^1\text{H}$  nuclei, and recovers some of the coupling information while still observing decoupled signals. Another sequence that provides similar information is the Attached Proton Test (APT). The major difference is that in APT the enhancement comes from the Nuclear Overhauser Effect (NOE) instead of polarization transfer. To maximize NOE it is important the decoupler is turned on as much as possible during the pulse sequence and acquisition. Below is the pulse sequence.



- Write the product operator notation for a  $^1\text{H}$ - $^{13}\text{C}$  coupled pair starting from  $K_z$ ; keep the delay time as a general variable,  $\tau$ .
- Sketch a plot of the intensity of the signal as a function of  $\phi$  in degrees (recall  $\phi = \pi J \tau$ ). For  $J = 125$  Hz, identify specific values of  $\tau$  that provide a maximum positive intensity, a maximum negative intensity, and zero intensity.

6.4. *Spectra*: Assign as many peaks as possible in spectra #13, 14, 18, and 19. Explain your reasoning. You may want to start your analysis with the advanced techniques used for spectra #15-17 and 20-22.

Present activity 6.1, 6.2, or 6.3 to a staff member, followed by a brief discussion.

## Oral Exam Checklist

1. Define the following terms as they apply to NMR spectroscopy:  $I$ ,  $m_I$ ,  $\gamma$ ,  $\mu$ ,  $P$ , Larmor frequency, and Zeeman effect. Discuss the possible values of  $I$  for a nucleus with a given number of protons and neutrons. Sketch the energy levels for a nucleus with a given value of  $I$  in an external magnetic field.
2. Sketch the energy levels for an  $AK$  system with a given relationship between  $\gamma_A$  and  $\gamma_K$ . Identify and label the transitions that can be driven using a pulse of EM radiation. Explain the labelling convention for the transitions. Explain how  $J$ -coupling affects the sketch. Discuss the individual terms that determine the position of a given energy level.
3. Explain the basic pulse-acquire experiment for acquiring data from the  $A$  nucleus of a heteronuclear  $AK$  system. Include descriptions of: 1) how the magnetization evolves due to the pulse, 2) how the magnetization evolves during acquisition, 3) how the FID is determined from the magnetization, and 4) how the observed lineshapes are determined from the position of the magnetization at the start of acquisition. Sketch a spectrum and explain the impact of  $\Delta_A$  and  $J$ .
4. For a given two-spin angular momentum basis operator: 1) calculate the matrix form of the operator, 2) correlate non-zero terms in the matrix with an energy level diagram, 3) demonstrate how the  $x$ -,  $y$ -, and  $z$ -components of classical vector models are determined from the matrix, and 4) sketch a classical vector representation of the operator.
5. For a given two-spin angular momentum basis operator: 1) write the product operator notation for acquiring data over time,  $t$ , from the operator, 2) correlate that description with a classical vector description, 3) sketch the spectrum, and 4) explain how decoupling impacts the analysis and the spectrum.
6. Design a pulse sequence to convert  $A_z$  to  $K_x$  for  $J = 50$  Hz and arbitrary values for  $\Delta_A$  and  $\Delta_K$ . Sketch the sequence and write the product operator description for these specific values of  $\Delta_A$ . Given a change in the phase of one of the pulses explain how to adjust the phase of the other pulses to compensate.
7. Design a 2D pulse sequence to correlate heteronuclear  $A$  and  $K$   $J$ -coupled nuclei with the following conditions: 1)  $f_1 = \Omega_A$ , 2)  $f_2 = \Omega_K$ , 3) start from  $A_z$  magnetization, and 4) the only observable term at the start of acquisition is  $K_x \cos(\Omega_A t_1)$ . Sketch and explain the pulse sequence, and write the corresponding product operator description.
8. Design a 2D pulse sequence to correlate heteronuclear  $A$  and  $K$   $J$ -coupled nuclei with the following conditions: 1)  $f_1 = \Omega_K$ , 2)  $f_2 = \Omega_A$ , 3) start from  $A_z$  magnetization, and 4) the only observable term at the start of acquisition is  $A_x \cos(\Omega_K t_1)$ . Sketch and explain the pulse sequence, and write the corresponding product operator description.
9. Sketch a set of vector diagrams for a given spin echo starting from a given operator. Use specified values for  $\theta$  and  $\phi$  rotations that occur for each  $\pi/2$  interval.
10. Discuss the impact of  $\gamma$  on the observed  $S/N$  in NMR spectra. Discuss how polarization transfer can improve the  $S/N$  of spectra when transferring magnetization from one nuclide to another with a lower value of  $\gamma$ . Discuss how the INEPT (or RINEPT) experiment accomplishes an improved  $^{13}\text{C}$  spectrum from transferring magnetization from attached  $^1\text{H}$  nuclei.
11. Describe how a 2D spectrum is acquired, processed, and analyzed.
12. Compare and contrast HETCOR with HSQC.